

# CAD increases the long noncoding RNA *PUNISHER* in small extracellular vesicles and regulates endothelial cell function via vesicular shuttling

Mohammed Rabiul Hosen,<sup>1,6</sup> Qian Li,<sup>1,2,6</sup> Yangyang Liu,<sup>1</sup> Andreas Zietzer,<sup>1</sup> Katharina Maus,<sup>1</sup> Philip Goody,<sup>1</sup> Shizuka Uchida,<sup>3</sup> Eicke Latz,<sup>4</sup> Nikos Werner,<sup>5</sup> Georg Nickenig,<sup>1</sup> and Felix Jansen<sup>1</sup>

<sup>1</sup>Heart Center Bonn, Molecular Cardiology, Department of Internal Medicine II, University Hospital Bonn, Rheinische Friedrich-Wilhelms University of Bonn Venusberg-Campus 1, 53127 Bonn, Germany; <sup>2</sup>Department of Cardiology, Second Hospital of Jilin University, 218 Ziqiang St., Changchun, China; <sup>3</sup>Center for RNA Medicine, Department of Clinical Medicine, Aalborg University, Frederikskaj 10B, 2, DK-2450 Copenhagen SV, Denmark; <sup>4</sup>Institute of Innate Immunity, University Hospital Bonn, University of Bonn, 53127 Bonn, Germany; <sup>5</sup>Department of Internal Medicine/Cardiology, Krankenhaus der Barmherzigen Brüder Trier, Nordallee 1, 54292 Trier, Germany

Long noncoding RNAs (lncRNAs) have emerged as biomarkers and regulators of cardiovascular disease. However, the expression pattern of circulating extracellular vesicle (EV)-incorporated lncRNAs in patients with coronary artery disease (CAD) is still poorly investigated. A human lncRNA array revealed that certain EV-lncRNAs are significantly dysregulated in CAD patients. Circulating small EVs (sEVs) from patients with (n = 30) or without (n = 30) CAD were used to quantify *PUNISHER* (also known as *AGAP2*-antisense RNA 1 [*ASI*]), *GAS5*, *MALAT1*, and *H19* RNA levels. *PUNISHER* (p = 0.002) and *GAS5* (p = 0.02) were significantly increased in patients with CAD, compared to non-CAD patients. Fluorescent labeling and quantitative real-time PCR of sEVs demonstrated that functional *PUNISHER* was transported into the recipient cells. Mechanistically, the RNA-binding protein, heterogeneous nuclear ribonucleoprotein K (hnRNPK), interacts with *PUNISHER*, regulating its loading into sEVs. Knockdown of *PUNISHER* abrogated the EV-mediated effects on endothelial cell (EC) migration, proliferation, tube formation, and sprouting. Angiogenesis-related gene profiling showed that the expression of vascular endothelial growth factor A (*VEGFA*) RNA was significantly increased in EV recipient cells. Protein stability and RNA immunoprecipitation indicated that the *PUNISHER*-hnRNPK axis regulates the stability and binding of *VEGFA* mRNA to hnRNPK. Loss of *PUNISHER* in EVs abolished the EV-mediated promotion of *VEGFA* gene and protein expression. Intercellular transfer of EV-incorporated *PUNISHER* promotes a pro-angiogenic phenotype via a *VEGFA*-dependent mechanism.

## INTRODUCTION

Coronary artery disease (CAD) and its cardiovascular sequelae represent the leading cause of mortality worldwide.<sup>1–4</sup> Emerging data suggest that noncoding RNAs (ncRNAs) are crucial regulators of pathological conditions, such as atherosclerosis. ncRNAs exert their

biological effects intracellularly but can also be released into the circulation.<sup>5,6</sup> Thus, circulating ncRNAs can provide useful information for the diagnosis of CAD as well as monitoring the progression of the disease,<sup>7</sup> which has recently been referred to as a liquid biopsy.<sup>8–10</sup> Although there are abundant ribonucleases in the bloodstream, ncRNAs remain relatively resistant to degradation. The stability of ncRNAs in plasma is mediated by their incorporation into and protection by extracellular vesicles (EVs) or through binding to exogenous proteins or lipids.<sup>11–13</sup>

MicroRNAs (miRNAs; ~22 nucleotides in length<sup>14</sup>) and long ncRNAs (lncRNAs; >200 nucleotides with no potential for translation into proteins<sup>15–17</sup>) are the most prominent kinds of ncRNAs.<sup>18</sup> We and others have demonstrated that circulating EV-incorporated miRNAs are significantly differentially regulated under pathological conditions and therefore are of high value for the diagnosis of cardiovascular disease.<sup>7,19–24</sup> However, miRNAs are not the most abundant ncRNAs within EVs.<sup>25</sup> Recent studies have highlighted that lncRNAs also participate in intercellular communication by way of EV-mediated cell-to-cell transfer. lncRNAs may exert their function by controlling gene expression in the nucleus or regulating other processes, such as RNA stability, in the cytoplasm.<sup>26–28</sup>

EVs are usually divided into two main classes according to their diameter: small EVs (sEVs; <150 nm) and large EVs (lEVs;

Received 30 November 2020; accepted 27 May 2021;  
<https://doi.org/10.1016/j.omtn.2021.05.023>.

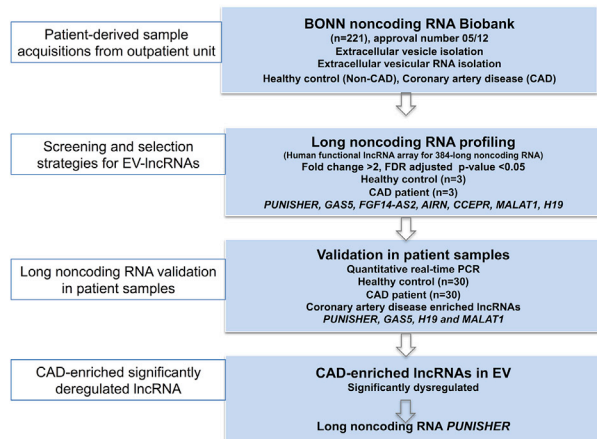
<sup>6</sup>These authors contributed equally

**Correspondence:** Mohammed Rabiul Hosen, PhD, Molecular Cardiology, Heart Center Bonn, Department of Internal Medicine II, Rheinische Friedrich-Wilhelms University Bonn, Venusberg-Campus 1, 53127 Bonn, Germany.  
**E-mail:** [hosenmr@uni-bonn.de](mailto:hosenmr@uni-bonn.de)

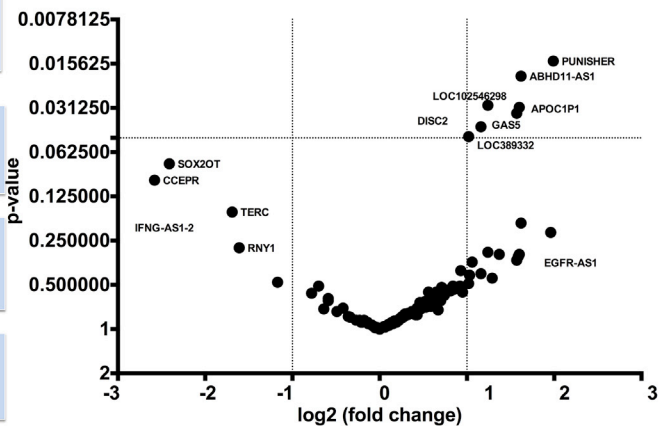
**Correspondence:** Felix Jansen, MD, PhD, Molecular Cardiology, Heart Center Bonn, Department of Internal Medicine II, Rheinische Friedrich-Wilhelms University Bonn, Venusberg-Campus 1, 53127 Bonn, Germany.  
**E-mail:** [felix.jansen@ukbonn.de](mailto:felix.jansen@ukbonn.de)



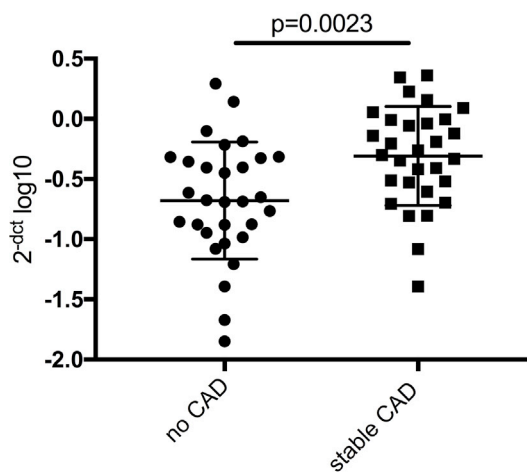
### A Workflow of clinical lncRNA study



### B Human long noncoding RNA array Non-CAD vs. CAD



### C sEV PUNISHER expression

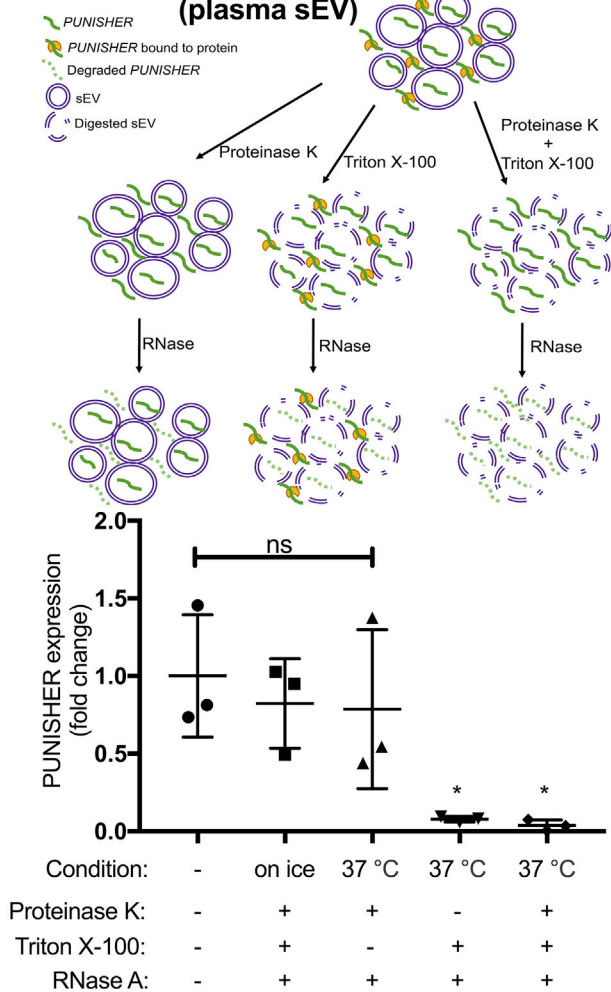


### D lncRNA analysis in plasma sEV

CAD (n=30) vs. no CAD (n=30)

lncRNA	Dysregulation	P value
PUNISHER	Stable CAD ↑	0.0023
GAS5	Stable CAD ↑	0.0251
H19	No difference	0.1508
MALAT1	No difference	0.1973

### E Vesicle-RNA degradation assay (plasma sEV)



(legend on next page)

150–1,000 nm).<sup>29</sup> Circulating sEVs and their molecular cargoes have recently emerged as promising diagnostic tools for various diseases including CAD.<sup>30</sup> Previous studies have provided evidence that circulating sEV are one of the main sources for lncRNAs in the bloodstream.<sup>31–34</sup> However, whether sEV-incorporated lncRNAs are differentially expressed in CAD and actively involved in disease progression is still poorly understood.

In the present study, we identified the sEV-incorporated lncRNA *PUNISHER* (also known as *AGAP2*-antisense RNA 1 [*AS1*]) as being significantly upregulated in CAD patients. *In vitro*, we found that *PUNISHER* can be selectively exported into sEVs via a heterogeneous nuclear ribonucleoprotein K (hnRNPk)-dependent mechanism. sEV-mediated intercellular transfer of *PUNISHER* increased the expression of vascular endothelial growth factor A (VEGFA) in recipient cells and promoted an angiogenic response. Our mechanistic studies indicate that *PUNISHER* exerts its function by interacting with the RNA-binding protein (RBP), hnRNPk, to regulate the expression of the proangiogenic protein VEGFA in endothelial cells (ECs).

## RESULTS

### Isolation and characterization of circulating sEV

A scheme of the workflow for the clinical lncRNA study is shown in Figure 1A. Circulating sEVs were isolated from the plasma of patients using a differential ultracentrifugation method (Figure S1A), as previously described.<sup>35</sup> sEVs isolated from plasma samples were characterized prior to the isolation of RNA. The sEVs were characterized according to the current recommendations of the International Society for Extracellular Vesicles (ISEV).<sup>35</sup> Immunoblotting analyses revealed that the isolated sEV expressed a distinct set of marker proteins, including CD9, CD81, and Syntenin1<sup>35,36</sup> (Figure S1B). Nanoparticle tracking analysis (NTA) showed that most of the isolated vesicles were 50–150 nm in diameter (Figure S1C), which is in line with the characteristic size (<150 nm) of sEVs.<sup>13</sup> Transmission electron microscopy (TEM) confirmed the size and morphology of the sEVs (Figure S1D).

### Identification of candidate lncRNAs

In order to explore whether sEV-incorporated lncRNAs are regulated differently in patients with or without CAD (non-CAD [NCAD]), a PCR-based human lncRNA array was performed in the screening cohort, which consisted of patients with stable CAD (n = 3) and NCAD (n = 3). The lncRNA array revealed a number of lncRNAs that were differentially expressed in sEVs. When thresholds of a >2-fold difference and a p value <0.05 were applied, the lncRNA

*PUNISHER* was shown to be significantly upregulated in CAD patients, along with several other lncRNAs (*ABHD11-AS1*, *GAS5*, *APOC1P1*, *DISC2*, etc.) (Figure 1B; Table S5). To validate the lncRNA array results, we prospectively studied another 60 patients, one-half with CAD (n = 30) and one-half NCAD (n = 30). Based on the results of the array and the well-known regulatory roles for certain lncRNAs in atherosclerosis, four lncRNAs (*MALAT1*,<sup>37,38</sup> *GAS5*,<sup>39,40</sup> *AGAP2-AS1* [*PUNISHER*],<sup>41</sup> and *H19*<sup>42,43</sup>) were selected for single quantitative real-time PCR (qRT (reverse transcriptase)-PCR) analysis in the validation cohort (Table S2).

### sEV-encapsulated lncRNA *PUNISHER* is upregulated in the plasma of CAD patients

Single qRT-PCR results showed that two of the lncRNAs had significantly higher expression levels in patients with stable CAD than patients with NCAD: *PUNISHER* (p = 0.0023; Figure 1C) and *GAS5* (p = 0.0251; Figure S2A). *H19* and *MALAT1* showed no significant differences between the two groups (Figures S2B and S2C). In summary, *PUNISHER* showed the most significant difference in expression levels between CAD and NCAD patients among the four lncRNAs studied (Figure 1D).

Baseline characteristics for the validation cohort are presented in Table 1. There was no significant difference with respect to age or gender between the two groups. Stable CAD patients were more frequently on low-dose aspirin and clopidogrel regimens (p = 0.005 and p = 0.001). The NCAD group had higher levels of high-density lipoprotein (HDL) cholesterol (p = 0.016), but other standard laboratory parameters were similar between the two groups (Table 1).

Comorbidities or medications have been shown to potentially affect the expression levels of sEV-bound ncRNAs.<sup>44</sup> A binary logistic regression analysis showed that higher or lower levels of *PUNISHER* were not significantly associated with any comorbidities. Furthermore, *PUNISHER* levels were found to be independent of the use of medications (Table S3).

To explore whether circulating extracellular *PUNISHER* is encapsulated into sEVs or bound to protein complexes, we performed a vesicle-RNA degradation assay. We found that digestion of proteins only (using proteinase K), before treatment with RNase, did not affect the levels of *PUNISHER* RNA. In contrast, treatment with Triton X-100, which acts as a detergent to disrupt the phospholipid membrane of vesicles, before treatment with RNase, led to an almost

**Figure 1. lncRNA expression in circulating small extracellular vesicles (sEVs) from patients with coronary artery disease (CAD) or without CAD (non-CAD [NCAD])**

(A) Schematic representation of the clinical long noncoding RNA (lncRNA) study. (B) Volcano plot showing differentially regulated human lncRNAs in sEVs derived from patient plasma by using a PCR-based human lncRNA array. Thresholds (dotted lines) of a 2-fold change and p values (false discovery rate [FDR] adjusted) <0.05 were set to distinguish the lncRNAs of interest; n = 3 for NCAD; n = 3 for CAD. (C) Expression of circulating sEV-associated *PUNISHER* was analyzed in NCAD (n = 30) and stable CAD (n = 30) patients by qRT-PCR. Values were normalized to *GAPDH* and expressed as  $2^{-[\text{CT}(\text{lncRNA}) - \text{CT}(\text{GAPDH})]}$   $\log_{10}$ . Data are presented as the mean  $\pm$  SD (p = 0.0023, by Student's t test). (D) List of the four lncRNAs analyzed in plasma sEV from the NCAD (n = 30) and stable CAD (n = 30) groups by qRT-PCR. (E) Top, a schematic representation of the vesicle-RNA degradation assays; bottom, plasma sEVs were treated in parallel using different conditions following RNase A digestion. *PUNISHER* was quantified by qRT-PCR (\*p < 0.05, compared with the untreated group; ns, not significant, n = 3, by 1-way ANOVA with Bonferroni correction for multiple comparisons test).

**Table 1. Baseline characteristics of the study population in the screening phase**

Characteristic	Total (n = 60)	NCAD (n = 30)	Stable CAD (n = 30)	p value
Age (year)	64.6 ± 10.7	63.8 ± 11.1	65.3 ± 10.4	0.584
Gender (no.; %)				0.542
Female	14 (23.3%)	8 (26.7%)	6 (20.0%)	
Male	46 (76.7%)	22 (73.3%)	24 (80.0%)	
Cardiovascular risk factors (%)				
Arterial hypertension	44 (73.3%)	23 (76.7%)	21 (70.0%)	0.559
Hyperlipoproteinemia	23 (38.3%)	11 (36.7%)	12 (40.0%)	0.791
Family history	13 (21.7%)	9 (30.0%)	4 (13.3%)	0.117
Diabetes	21 (35.0%)	11 (55.0%)	10 (33.3%)	0.524
Smoking	17 (28.3%)	7 (23.3%)	10 (33.3%)	0.390
Body mass index, kg/m <sup>2</sup>	27.4 ± 3.9	27.2 ± 4.6	27.7 ± 3.0	0.655
Medical history (%)				
Previous bypass	0 (0%)	0 (0%)	0 (0%)	1.000
Previous MI (6 months)	0 (0%)	0 (0%)	0 (0%)	1.000
Previous stroke	2 (3.3%)	2 (6.7%)	0 (0%)	0.150
Chronic kidney disease	2 (3.3%)	1 (3.3%)	1 (3.3%)	1.000
PCI				
Previous	36 (60%)	18 (43.3%)	23 (76.7%)	0.008
Coronary artery disease (no.; %)				0.001
1 vessel	3 (5.0%)	0 (0%)	3 (10.0%)	
2 vessels	12 (20.0%)	0 (0%)	12 (40.0%)	
3 vessels	13 (21.7%)	0 (0%)	13 (43.3%)	
Medication on administration (no.; %)				
ACE inhibitors	42 (70.0%)	18 (60.0%)	24 (80.0%)	0.091
Angiotensin receptor blockers	11 (18.3%)	5 (16.7%)	6 (20.0%)	0.739
Beta blockers	51 (85.0%)	25 (83.3%)	26 (86.7%)	0.718
Calcium channel blockers	10 (16.7%)	5 (16.7%)	5 (16.7%)	1.000
Diuretics	24 (40.0%)	13 (43.3%)	11 (36.7%)	0.598
Statins	48 (80.0%)	20 (66.7%)	28 (93.3%)	0.010
Nitrates	4 (6.7%)	2 (6.7%)	2 (6.7%)	1.000
Aspirin	47 (78.3%)	19 (63.3%)	28 (93.3%)	0.005
Clopidogrel	10 (16.7%)	0 (0%)	10 (33.3%)	0.001
Laboratory parameters				
Glucose	120.7 ± 60.3	116.3 ± 37.2	125.2 ± 77.8	0.583
Hb A1c (%)	6.8 ± 3.9	6.1 ± 0.7	7.5 ± 5.4	0.179
Serum creatinine (mg/dL)	1.0 ± 0.3	1.0 ± 0.4	1.0 ± 5.4	0.637
Glomerular filtration rate (mL/min)	65.6 ± 10.3	65.4 ± 11.1	65.7 ± 9.5	0.913
Triglycerides (mg/dL)	131.2 ± 76.3	120.5 ± 48.7	142.2 ± 96.7	0.278

(Continued)

**Table 1. Continued**

Characteristic	Total (n = 60)	NCAD (n = 30)	Stable CAD (n = 30)	p value
Cholesterol (mg/dL)	176.6 ± 49.4	186.5 ± 54.0	166.6 ± 42.9	0.121
HDL cholesterol (mg/dL)	50.5 ± 14.9	55.1 ± 16.4	40.6 ± 11.8	0.016
LDL cholesterol (mg/dL)	106.0 ± 35.2	110.3 ± 39.5	101.7 ± 31.3	0.349
C-reactive protein (mg/L)	5.9 ± 10.8	5.3 ± 9.4	6.5 ± 12.3	0.665
Leukocytes (10 <sup>9</sup> /L)	7.3 ± 2.1	7.2 ± 1.9	7.5 ± 2.3	0.600

Continuous variables are presented as the mean ± SD, and categorical variables are presented as the percentage of patients. NCAD, non-coronary artery disease; stable CAD, stable coronary artery disease; MI, myocardial infarction; PCI, percutaneous coronary intervention; ACE, angiotensin-converting enzyme; Hb A1c, hemoglobin A1c; LDL, low-density lipoprotein; HDL, high-density lipoprotein. Chronic kidney disease was defined as a glomerular filtration rate <60 mL/min.

complete degradation of *PUNISHER* RNA. These findings indicate that the circulating extracellular *PUNISHER* is primarily incorporated into sEVs, which protect the RNA from resident nucleases (Figure 1E). Additionally, we investigated the stability of the *PUNISHER* transcript in sEVs isolated from freshly collected plasma versus plasma stored at  $-80^{\circ}\text{C}$  for 5 years. There was no significant difference in *PUNISHER* expression levels between the two groups (Figure S2D), confirming the stability of ncRNAs in frozen plasma over several years, if stored correctly.<sup>45</sup>

#### Atherosclerotic stimuli cause endothelial sEV to be enriched in *PUNISHER* *in vitro*

Because we found that sEVs containing *PUNISHER* were significantly upregulated in patients with CAD, and previous studies show that *PUNISHER* is an endothelial-specific lncRNA,<sup>41,46</sup> we next explored whether pro-atherosclerotic conditions might regulate cellular or sEV-incorporated *PUNISHER* expression levels *in vitro*. First, EC-derived sEVs were isolated from human coronary artery ECs (HCAECs) through a series of differential ultracentrifugation steps, as previously described (Figure S2A). The resulting sEVs were characterized by immunoblotting for sEV marker expression, NTA for size distribution, and TEM for morphology (Figures S3A–S3C). To confirm that *PUNISHER* is expressed primarily in the heart, expression profiling of *PUNISHER* in eight major human tissues was performed by using qRT-PCR on commercially available cDNA from eight different tissues (major organs) of human origin (Human Total RNA Master Panel II; Clontech; #636643) (Figure S3D). The origins of *PUNISHER*-enriched vesicles were investigated further by the utilization of different vascular cells (vascular smooth muscle cells, HCAECs, and human umbilical vein endothelial cells [HUVECs]), as well as immune cells, such as platelets. Interestingly, we found that the lncRNA *PUNISHER* is enriched in ECs and their corresponding sEVs (Figure S3E).<sup>41</sup> The expression of *PUNISHER* in HCAECs and the corresponding sEVs was confirmed by qRT-PCR (Figure S4A). Recent investigations indicated that oxidized low-density

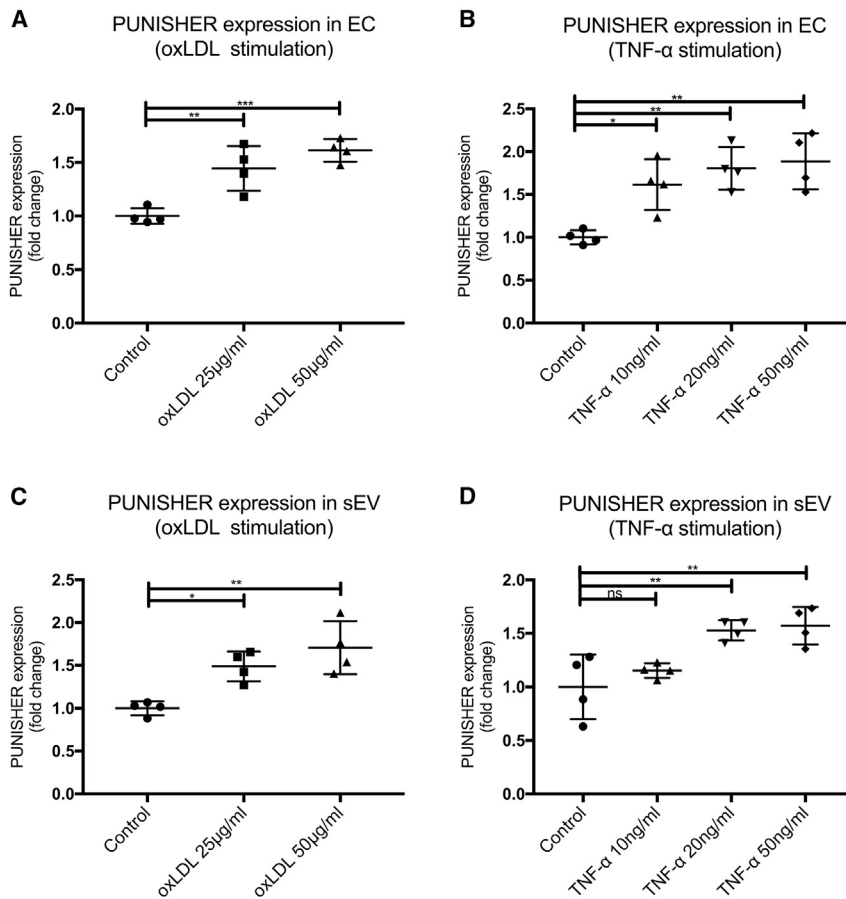


**Figure 2. Atherosclerotic stimuli increase *PUNISHER* expression in endothelial cells (ECs) and corresponding sEVs *in vitro***

(A and B) *PUNISHER* was analyzed in ECs upon stimulation with different concentrations of oxidized low-density lipoprotein (oxLDL) or tumor necrosis factor  $\alpha$  (TNF- $\alpha$ ) by using qRT-PCR (\* $p < 0.05$ , \*\* $p < 0.01$ , \*\*\* $p < 0.001$ ,  $n = 4$ , by 1-way ANOVA with Bonferroni correction for multiple comparisons test). (C and D) *PUNISHER* was analyzed in sEVs following stimulation with different concentrations of oxLDL or TNF- $\alpha$  by using qRT-PCR. Cycle of threshold (CT) values were normalized to GAPDH, and expression was depicted as fold change (\* $p < 0.05$ , \*\* $p < 0.01$ ,  $n = 4$ , by 1-way ANOVA with Bonferroni correction for multiple comparisons test). Data represent the mean  $\pm$  SD.

### *PUNISHER* exerts its function via interaction with the RBP hnRNPK

We next aimed to study the mechanism that regulates the enrichment of *PUNISHER* within sEVs. Recently, RBPs have been shown to be important regulators of the packaging and sorting of ncRNAs into EV.<sup>52–54</sup> However, thus far, there is little known about the mechanisms of packaging lncRNAs into endothelial sEVs. To investigate the molecular mechanism of ncRNA packaging, we re-analyzed our previously published proteomic analysis of EVs.<sup>54</sup> We found that a significant portion of the protein candidates that were identified were annotated as RBPs, according to the SwissProt database. In

particular, hnRNPs were prominently expressed in isolated EVs, including hnRNPA2B1, hnRNPU, and hnRNPK, as previously published by our group.<sup>54</sup>

hnRNPs are a large family of RBPs that have been reported to mediate the loading of ncRNAs into EV.<sup>53,55</sup> To examine whether the packaging of *PUNISHER* into EVs is mediated by hnRNPs, we utilized publicly available online tools to predict *PUNISHER*-hnRNP interaction partners by using the catRAPID omics algorithm.<sup>56</sup> In this way, we identified hnRNPK as the top-ranked potential interaction partner for *PUNISHER in silico* (Table S4). We performed a cross-linked RNA immunoprecipitation (RIP) experiment by using an antibody against hnRNPK in ECs and sEVs to experimentally confirm the binding between *PUNISHER* and hnRNPK (Figures 3A–3C). Interestingly, qRT-PCR analysis revealed that the interaction of hnRNPK with *PUNISHER* is specific, and no other lncRNAs (*GAS5*, *MALAT1*, and *H19*) are enriched in either EC or sEVs from the RIP experiments (Figures 3A and 3B). To further investigate whether hnRNPK interacts with other lncRNAs that were upregulated in our clinical samples, we used the RNA Interactome (RNAInter) database to make an *in silico* prediction of the interaction of hnRNPK with lncRNAs, based on the coverage score. We found that *PUNISHER* and *MALAT1* are predicted to bind to hnRNPK, but not *H19* and *GAS5*, based on

lipoprotein (oxLDL) or tumor necrosis factor alpha (TNF- $\alpha$ ) plays pivotal roles in the development of atherosclerosis and endothelial dysfunction, and they are extensively used *in vitro* and *in vivo* as atherosclerotic stimuli.<sup>47–51</sup> Intriguingly, stimulation with oxLDL or TNF- $\alpha$  caused significant upregulation of *PUNISHER* levels, both in the parental ECs and in EC-derived sEVs, without affecting the overall number of sEVs (Figures 2A–2D; Figure S4B).

Based on the current annotation, *AGAP2-AS1* (also known as *PUNISHER*) is an RNA gene, which has been categorized to the ncRNA class. Unlike protein-coding genes, *PUNISHER* does not contain any obvious open reading frame (ORF).<sup>41</sup>

By definition, the lncRNA *PUNISHER* is not translated into a protein. *In silico* predictions of the protein-coding potential of *PUNISHER* indicate that it is a bona fide lncRNA that does not encode proteins. Since the subcellular localization of a given transcript may be considered an important clue about its function, we investigated *PUNISHER* localization and demonstrated that *PUNISHER* is localized to both the cytosol and nucleus by fractionating the RNA followed by qRT-PCR-based quantification. Intriguingly, *PUNISHER* is highly enriched in the cytosolic fraction, compared to the nuclear fraction, of ECs (Figure S5A).

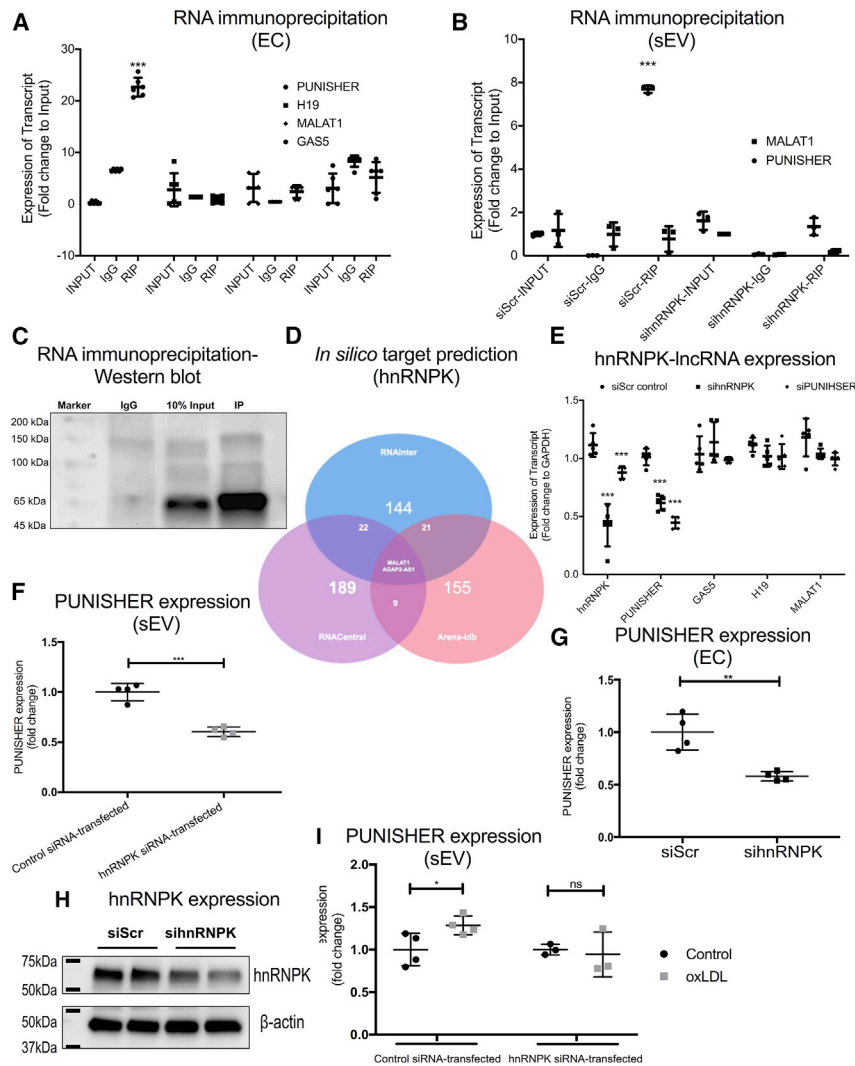


**Figure 3. Interaction between *PUNISHER* and heterogeneous nuclear ribonucleoprotein K (hnRNPK) mediates *PUNISHER* packaging into sEVs**

(A) Cross-linked RNA immunoprecipitation (RIP) experiments followed by qRT-PCR quantification was performed to confirm the reciprocal binding of *PUNISHER*, *MALAT1*, *H19*, and *GAS5* to hnRNPK in human ECs. From the RIP experiments, strong binding of hnRNPK was observed in comparison to IgG (negative control). Quantification was performed by normalizing the values with the inputs (10%). Data represent the mean  $\pm$  SD (\*\* $p < 0.001$ ,  $n \geq 4$ , by Student's *t* test). (B) RIP experiments in sEV lysates followed by qRT-PCR quantification were performed to confirm the binding of *PUNISHER*, *MALAT1*, *H19*, and *GAS5* in sEVs. Data represent the mean  $\pm$  SD (\*\* $p < 0.001$ ,  $n \geq 4$ , by Student's *t* test). (C) Immunoprecipitation (IP) of hnRNPK followed by western blotting confirmed the reciprocal binding of hnRNPK to *PUNISHER*. The respective IgG antibody from the same species was used as an IP negative control. The enrichment was confirmed with input (10%) from the cellular lysates. (D) *In silico* target prediction of hnRNPK by using publicly available tools, based on the coverage score, by using RNAInter,<sup>57</sup> RNAcentral,<sup>58</sup> and Arena-ldb<sup>59</sup> databases. Based on their interaction scores, only *MALAT1* and *AGAP2-AS1* (*PUNISHER*) are predicted to bind to hnRNPK. (E) Expression levels of several lncRNAs (*PUNISHER*, *MALAT1*, *H19*, and *GAS5*) upon silencing of *PUNISHER*/hnRNPK in ECs by using siRNAs (\*\* $p < 0.001$ ,  $n = 4$ , by Student's *t* test). (F and G) Expression of *PUNISHER* upon silencing of hnRNPK in ECs and their corresponding sEVs by using siRNA (\*\* $p < 0.001$ ,  $n = 4$ , by Student's *t* test). (H) Western blot analysis of hnRNPK protein expression was performed on the hnRNPK siRNA- or control siRNA-transfected ECs.  $\beta$ -actin was used as a marker. hnRNPK protein levels were assessed using ImageJ image analysis software (\*\* $p < 0.01$ ,  $n = 4$ , by Student's *t* test). (I) Prior to oxLDL treatment, ECs were transfected with hnRNPK siRNA or control siRNA. *PUNISHER* expression was analyzed in the corresponding sEVs by qRT-PCR. *GAPDH* was used as an endogenous control (\* $p < 0.05$ ,  $n = 3-4$ , by Student's *t* test).

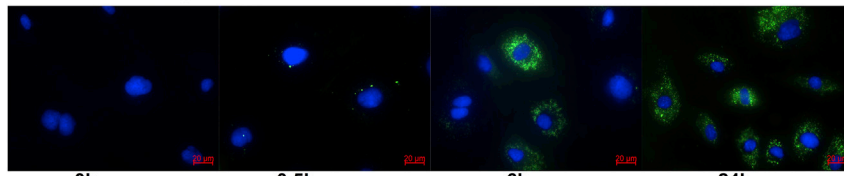
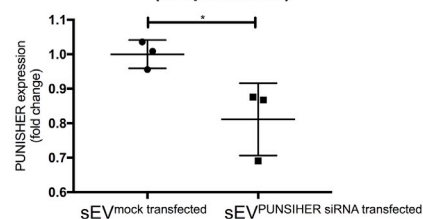
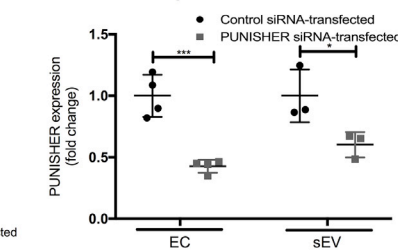
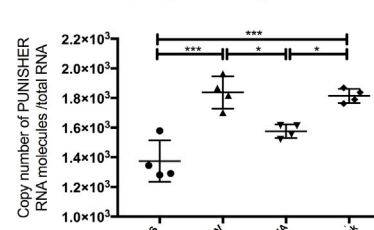
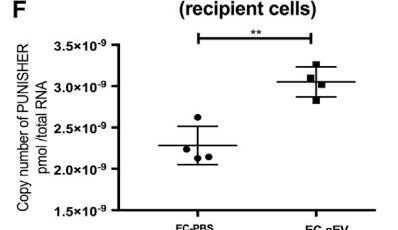
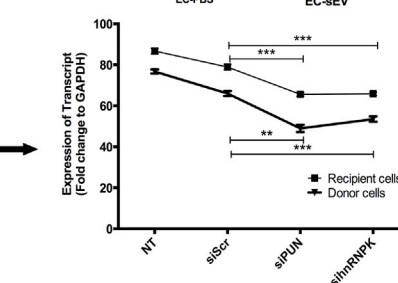
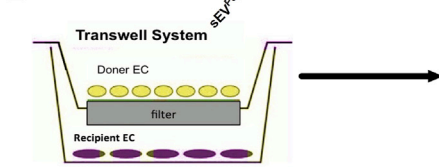
the high-interaction scores that they give<sup>57</sup> and compared with other databases (Figure 3D; Table S6).<sup>58,59</sup>

We then evaluated the effect of hnRNPK knockdown on sEV-incorporated *PUNISHER* levels and other lncRNA expression in ECs (Figure 3E). We found that upon hnRNPK knockdown in EC, the expression of *PUNISHER* is reduced, whereas other lncRNAs remain unchanged, suggesting that the interaction of hnRNPK to *PUNISHER* is specific (Figure 3E). Importantly, hnRNPK depletion reduced the levels of *PUNISHER* in ECs and the corresponding sEVs (Figures 3F-3H), demonstrating that hnRNPK may participate in the loading of *PUNISHER* into sEVs. Furthermore, *in vitro* atherosclerotic stimulus, oxLDL-induced *PUNISHER* upregulation within sEVs, was abrogated upon hnRNPK knockdown, which confirms the importance of hnRNPK-mediated *PUNISHER* packaging under atherosclerotic conditions (Figure 3H; Figure S5B). Loss of *PUNISHER* and

hnRNPK function leads to a reduction of *PUNISHER* and hnRNPK mRNA level in the corresponding sEVs, but no significant effects were observed in the case of other lncRNAs, namely, *GAS5*, *H19*, and *MALAT1*, further suggesting that hnRNPK is an interaction partner for *PUNISHER* and regulates the packaging of ncRNA into sEVs (Figure 3I). In summary, our data clearly indicate that hnRNPK is an interaction partner for *PUNISHER*, which may regulate the loading of *PUNISHER* into sEVs.

#### sEV-incorporated *PUNISHER* regulates target EC function

Increasing evidence suggests that sEVs act as a vehicle for the intercellular transfer of their contents to modulate the fate of recipient cells.<sup>39,53,60,61</sup> Because circulating sEV-containing *PUNISHER* might exert its main biological effect on target ECs, we first investigated whether endothelial-derived sEVs could deliver *PUNISHER* into target ECs. By co-incubating sEVs and ECs, we observed a

**A sEV transfer experiment****B PUNISHER expression (recipient cells)****C PUNISHER expression in EC/sEV****D PUNISHER expression (recipient cells)****F PUNISHER expression (recipient cells)****E Transwell System**

time-dependent internalization of sEVs into the recipient ECs (Figure 4A). The transfer of *PUNISHER* into target ECs was diminished using *PUNISHER*-downregulated sEVs (sEV<sup>*PUNISHER* downregulated</sup>), which were generated from ECs following transfection with *PUNISHER* small interfering RNAs (siRNAs) (Figure 4B). The efficiency of *PUNISHER* downregulation following siRNA transfection was confirmed using qRT-PCR in ECs and the corresponding sEVs (Figure 4C), without affecting other lncRNAs (Figures S6A–S6C). An qRT-PCR-based absolute quantification assay in target ECs confirmed the efficient delivery of *PUNISHER* by sEV (Figure S6D); furthermore, compared with sEVs, sEV<sup>*PUNISHER* downregulated</sup> transferred less *PUNISHER* into the recipient ECs (Figures 4D–4F). Moreover, to distinguish between endogenous and exogenously delivered *PUNISHER*, we performed copy number analysis on *PUNISHER*-downregulated recipient ECs. The results demonstrated that sEV transfer could rescue the reduced level of *PUNISHER* in *PUNISHER*-silenced target ECs (Figure 4E; Figure S6D). To confirm whether sEV-mediated *PUN-*

**Figure 4. sEV-incorporated *PUNISHER* is transferred into recipient ECs**

(A) PKH67-labeled sEVs (green) were cultured with recipient ECs for 0, 0.5, 6, and 24 h. The nuclei of the cells were stained with 4',6-diamidino-2-phenylindole (DAPI; blue), and images were taken by using immunofluorescence microscopy. Scale bar, 20  $\mu$ m. (B) *PUNISHER* expression was assessed in target ECs that were treated with sEV<sup>*PUNISHER* downregulated</sup> or sEV<sup>mock</sup> transfected using qRT-PCR. CT values were normalized to *GAPDH* and were expressed as fold change (\* $p < 0.05$ ,  $n = 3$ , by Student's t test). (C) *PUNISHER* expression was analyzed in *PUNISHER*-siRNA- or control-siRNA-transfected ECs and the corresponding sEVs by qRT-PCR. *GAPDH* was used as an endogenous control (\* $p < 0.05$ , \*\*\* $p < 0.001$ ,  $n = 3-4$ , by Student's t test). (D–F) *PUNISHER* expression was assessed in target ECs that were treated with PBS, sEVs, sEV<sup>*PUNISHER* downregulated</sup>, or sEV<sup>mock</sup> transfected using copy number analysis (\* $p < 0.05$ , \*\*\* $p < 0.001$ ,  $n = 4$ , by 1-way ANOVA with Bonferroni multiple comparisons test). (E) Transwell experiments with normal, siScr, si*PUNISHER*, and sihrRNPk in donor cells and recipient cells. *PUNISHER* expression was quantified in donor and target ECs that were treated with sEVs from cells transfected with siRNAs. *GAPDH* was used as a control. (\*\* $p < 0.01$ , \*\*\* $p < 0.001$ , Student's t test). HCAECs, human coronary artery ECs.

*ISHER* transfer exists *in vitro*, we established a Transwell-based experiment by utilizing *PUNISHER*-/hrRNPk-silenced donor cells and comparing them with control ECs. We observed that the sEVs have the potential to deliver *PUNISHER* to the recipient cells. These data indicate that there is reduced transfer of *PUNISHER* from both *PUNISHER*- and hrRNPk-silenced donor cells into the corresponding recipient ECs via sEV and suggest that hrRNPk is involved in EV-mediated *PUNISHER* transfer.

Next, we investigated the function of sEV-incorporated *PUNISHER*. Because *PUNISHER* has been shown to be a major regulator of EC function,<sup>41</sup> we investigated whether the *PUNISHER* RNA found in sEVs can directly affect target EC migration, proliferation, *in vitro* sprouting, and network formation. Treatment of target ECs with sEVs caused an increase in EC migration (Figure 5A; Figure S7A), proliferation (Figures 5B and 5C), and network formation (Figures 5D and 5E; Figures S7B and S7C), whereas *PUNISHER* silencing reduces *in vitro* sprouting of ECs (Figures 5F and 5G). Importantly, sEV-mediated effects on the recipient ECs were abolished when sEV<sup>*PUNISHER* downregulated</sup> were used, indicating that the *PUNISHER* found in the sEVs regulates target EC function and phenotypes by promoting angiogenic responses. Consistent with these findings, the downregulation of *PUNISHER* in ECs resulted in reduced migration (Figures S8A and S8B), proliferation (Figure S8C), and network formation (Figures S8D–S8G).

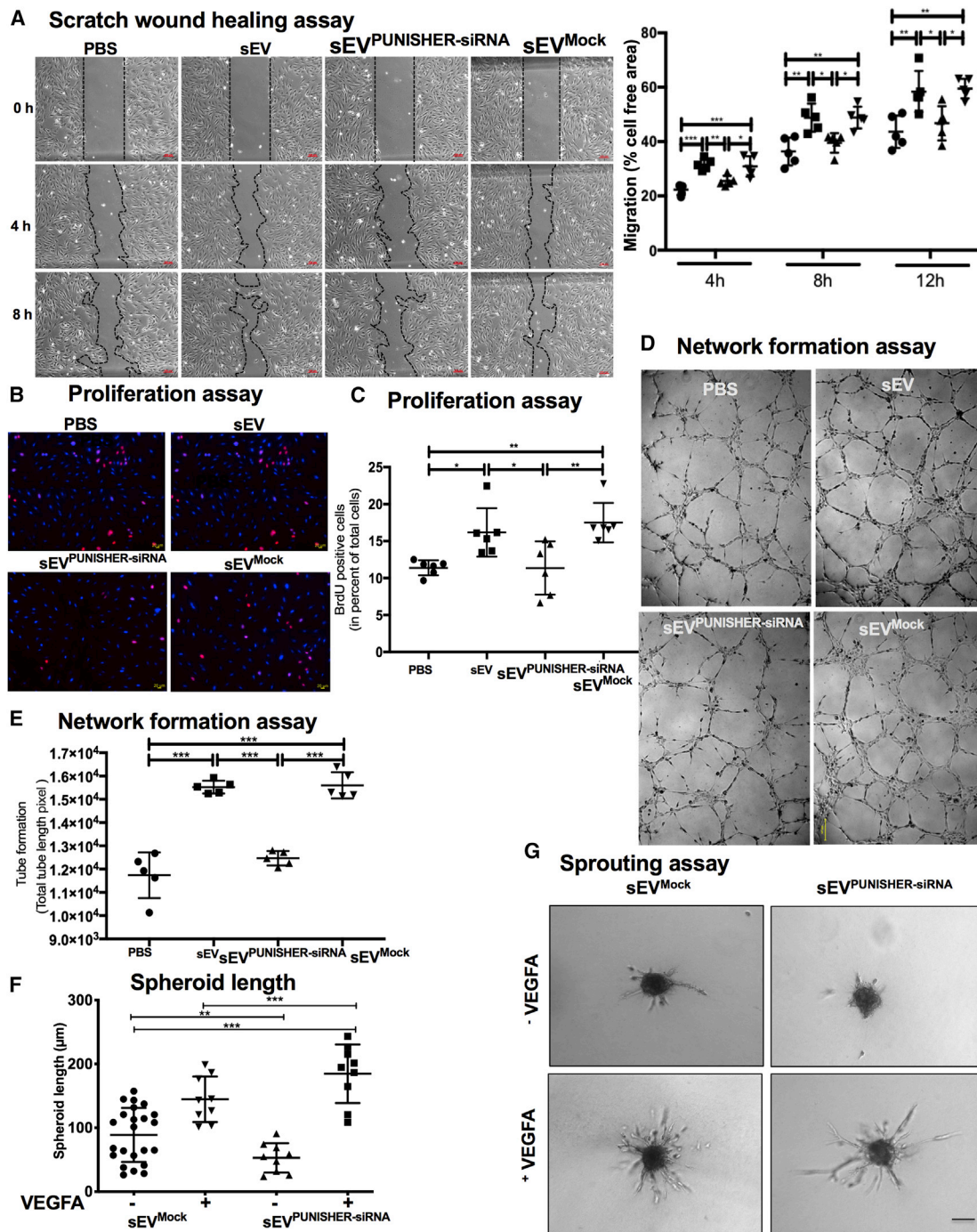


**Figure 5. PUNISHER in sEVs regulates target EC function**

sEV<sup>PUNISHER</sup> downregulated and sEV<sup>Mock</sup> transfected were separately derived from parent ECs transfected with PUNISHER siRNA or control siRNA. ECs were co-incubated with sEVs, sEV<sup>PUNISHER</sup> downregulated, sEV<sup>Mock</sup> transfected, or vehicle. (A) A scratch-migration assay was performed, and representative images of cells migrating into the scratched region after 0, 4, and 8 h are shown. Quantitative analysis of the migration was measured as a percentage of total cell-free area (\*p < 0.05, \*\*p < 0.01, \*\*\*p < 0.001, n = 5, by 1-way ANOVA with Bonferroni multiple comparisons test). Scale bars, 100 µm. (B and C) Bromodeoxyuridine (BrdU) incorporation was determined by immunofluorescence (red). Nuclei were stained with DAPI (blue). The percentage of BrdU-positive cells was compared with the total number of cells (\*p < 0.05, \*\*p < 0.01, n = 6, by 1-way ANOVA with Bonferroni's multiple comparisons test). Scale bars, 20 µm; 100× magnification. (D and E) Network formation assays of ECs. Capillary tubes were imaged with an

(legend continued on next page)



### sEV-mediated transfer of *PUNISHER* regulates VEGFA transcripts in recipient ECs

To explore the underlying mechanism of *PUNISHER* (delivered via sEVs) for the regulation of angiogenic functions in the recipient ECs, we used two independent experimental approaches: (1) direct downregulation of *PUNISHER* expression in ECs using siRNAs (*PUNISHER* siRNA versus control siRNA) and (2) treatment of recipient ECs with sEVs in which *PUNISHER* has been downregulated (sEV<sup>*PUNISHER* downregulated</sup> versus sEV<sup>mock transfected</sup>). An RT<sup>2</sup> Profiler PCR array, which covers 84 key genes that are involved in modulating the biological processes of angiogenesis, was performed on both of the above-mentioned models. In the cellular model of *PUNISHER* knockdown, analysis of the array results revealed that a series of pro-angiogenic genes, including pro-inflammatory factors (interleukin 1 beta [IL-1 $\beta$ ], IL-6, and TNF- $\alpha$ ), as well as other cellular factors (chemokines, vascular endothelial factors), were significantly downregulated (Figure 6A). When ECs were treated with sEV<sup>*PUNISHER* downregulated</sup> and compared with sEV<sup>mock transfected</sup>, the array results showed that the anti-angiogenic C-X-C motif chemokine 10 (CXCL10) was upregulated, and four pro-angiogenic genes were downregulated by at least 2-fold, namely jagged1 (JAG1), matrix metalloproteinase-2 (MMP-2), angiopoietin 4 (ANGPT4), and VEGFA (Figure 6B). Interestingly, when the overall angiogenesis gene-expression profile was compared between the two models, VEGFA, a well-known, potent pro-angiogenic factor,<sup>62</sup> was found to be decreased upon downregulation of *PUNISHER* in both arrays (Figures 6A and 6B).

To confirm the above findings, single qRT-PCR, immunoblotting, and enzyme-linked immunosorbent assay (ELISA) were performed. Notably, *PUNISHER* downregulation in ECs resulted in a reduction in VEGFA expression on both the mRNA (Figure 6E) and protein levels (Figure 6G; Figure S9A). Besides this, we also analyzed the expression of another dysregulated gene, CXCL10, in donor and recipient cells (Figures S9D and S9E). In line with these findings, ECs treated with sEV<sup>*PUNISHER* downregulated</sup> showed reduced expression of VEGFA mRNA (Figure 6F), protein (Figure 6H; Figure S9B), and in the cellular supernatants (Figures 7A and 7B) compared to sEV<sup>mock transfected</sup>. Furthermore, upon *PUNISHER* knockdown, although VEGFA mRNA was downregulated in the parent and recipient ECs (Figure 6E; Figure 7B), VEGFA mRNA was not significantly decreased in the corresponding sEVs (sEV<sup>*PUNISHER* downregulate</sup>) (Figures S9B and S9C). These data exclude the possibility of VEGFA mRNA transfer via sEVs but instead raise a question: how does *PUNISHER* regulate mRNA expression or protein synthesis of VEGFA? To explore this mechanistically, we performed hnRNPK immunoprecipitation (IP) and RIP experiments using EC cellular lysates, which confirmed that hnRNPK is an interaction partner for *PUNISHER*. hnRNPK has been reported to bind to the 3' UTR (untranslated re-

gion) of mRNA, to post-transcriptionally regulate its levels by regulating its stability,<sup>63–66</sup> and is known to regulate the angiogenesis pathway by acting as a transcriptional activator of VEGF.<sup>63</sup> To confirm this, we performed RIP followed by qRT-PCR (RIP-qPCR), which indicated a reduction in VEGFA mRNA binding to hnRNPK. Although enrichment of VEGFA mRNA in *PUNISHER*- or hnRNPK-silenced cells is comparable with scramble control short-interfering RNA (siScr)-treated cells, a lower level of enrichment was recorded in both cells (Figure 7C). To examine whether such binding has any effect on the transcript stability of VEGFA upon *PUNISHER* silencing, we treated cells with actinomycin D (5  $\mu$ g/mL) to inhibit RNA synthesis and measured the VEGFA expression profile via qRT-PCR. Interestingly, we observed that the expression of the VEGFA transcript is downregulated in *PUNISHER*-silenced cells, in comparison to siScr-treated cells, suggesting that *PUNISHER* may regulate VEGFA transcription (Figure 7D). Next, to experimentally validate the involvement of hnRNPK in the post-translational regulation of VEGFA, cycloheximide (CHX; an inhibitor of protein synthesis)-mediated protein stability assays were performed upon *PUNISHER* silencing, and the stability of cellular VEGFA was detected (Figure 7E). In addition, we investigated whether impairment of the angiogenic response in *PUNISHER*-silenced ECs and recipient ECs can be rescued by exogenous supplementation with the VEGFA protein. To address this point, we performed a recipient EC network formation assay, with or without VEGFA supplementation. Our rescue experiments revealed that the angiogenic activity in EC receiving EVs from *PUNISHER*-silenced cells can only be rescued by adding a high concentration of extracellular VEGFA (5,000 pg/mL; Figure S10) but not with a lower concentration (500 pg/mL; data not shown). This result excluded that there are different levels of VEGFA mRNA transport by EVs (Figure 7F).

## DISCUSSION

Circulating ncRNAs are a novel class of biomarkers in cardiovascular disease.<sup>7,67</sup> Previous studies have highlighted that circulating EVs are one of the major vehicles for ncRNAs in the bloodstream, providing protection from circulating RNases and promoting stability in the plasma.<sup>7,68</sup> Previously, we found that EV-incorporated, but not freely circulating, ncRNAs (*miRNA-126* and *miRNA-199a*) could predict the occurrence of cardiovascular events in patients with stable CAD.<sup>69</sup> Thus far, miRNAs and lncRNAs are the most prominent and well-characterized ncRNAs. However, there is evidence that miRNAs are not the most abundant ncRNAs in EVs.<sup>70,71</sup> Whereas EV-incorporated miRNAs have already been characterized in a number of studies, the function of EV-incorporated lncRNAs, especially in CAD, is largely unknown. Moreover, in the bloodstream, the quantity of lncRNAs in sEVs is higher than in other types of EVs.<sup>72</sup> In this

---

immunofluorescence microscope. Total tube length was measured and quantitated by using ImageJ image analysis software (NIH, USA; \*\*p < 0.01, \*\*\*p < 0.001, n = 6, by 1-way ANOVA with Bonferroni multiple comparison test). Scale bar, 200  $\mu$ m. (F and G) *In vitro* sprouting assay in which ECs are co-incubated with sEVs with or without vascular endothelial growth factor A (VEGFA; 5  $\mu$ g/mL), sEV<sup>*PUNISHER* downregulated</sup>, or sEV<sup>mock transfected</sup>. Cumulative sprouting length was measured and quantitatively analyzed using digital imaging analysis software (AxioVision Rel. 4.8; Carl Zeiss; \*\*\*p < 0.001, n = 6, by 1-way ANOVA with Bonferroni multiple comparisons test). Scale bar, 200  $\mu$ m.

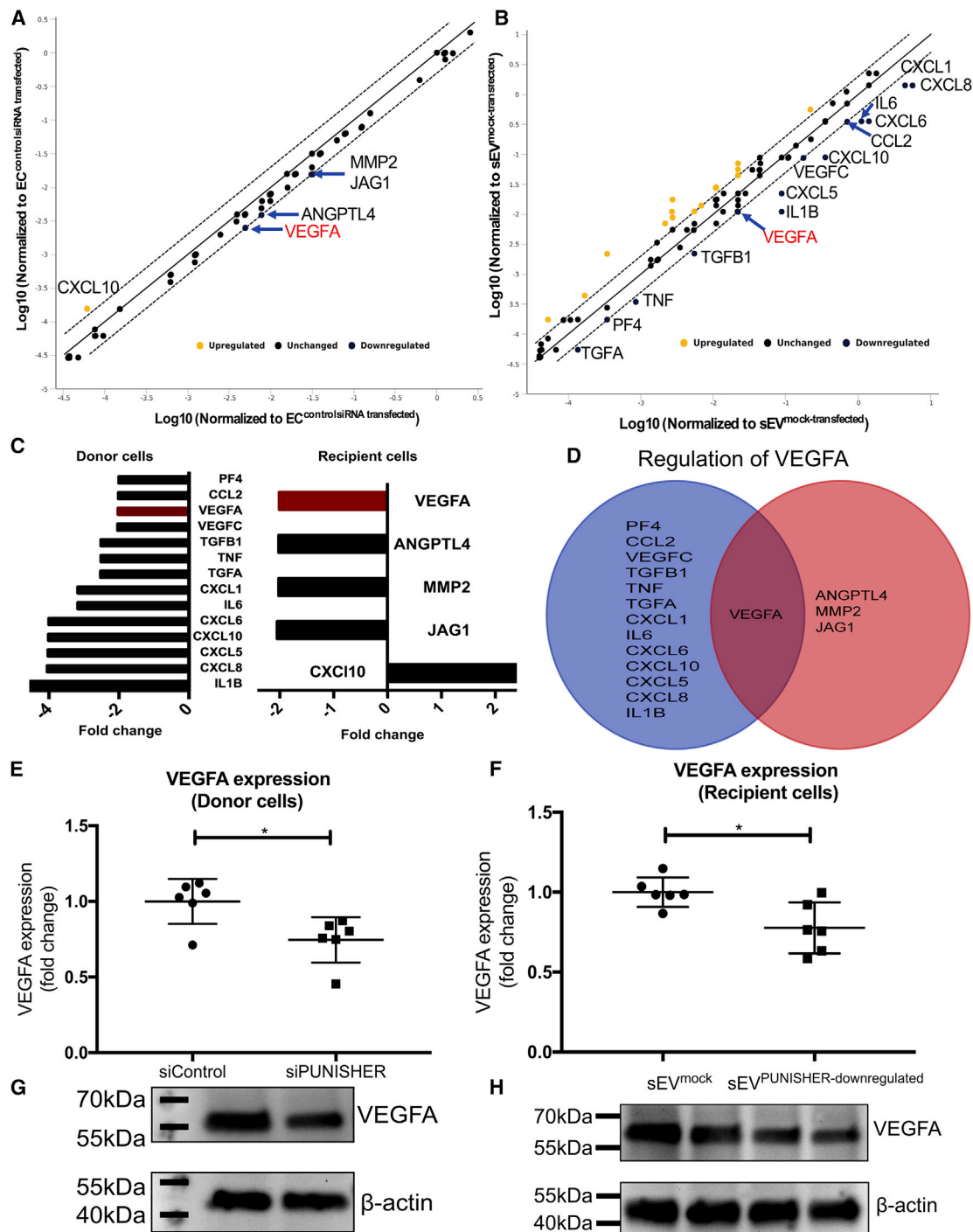


**Figure 6. sEV-mediated transfer of PUNISHER RNA regulates the level of VEGFA in recipient ECs**

RT<sup>2</sup> Profiler PCR array analyses (angiogenesis) were performed on ECs treated with PUNISHER siRNA and control siRNA-transfected ECs (n = 3). The same array was performed on ECs treated with sEV<sup>mock-transfected</sup> or sEV<sup>PUNISHER-downregulated</sup> (n = 3). Ribosomal protein lateral stalk subunit P0 (RPLP0; as PCR array control) was used as an endogenous control in the PCR array. (A) A scatterplot shows the differentially regulated genes between PUNISHER knockdown and control ECs by PCR array. The downregulated genes with a >2-fold change are labeled and listed. (B) A scatterplot shows the differentially regulated genes in target ECs after sEV<sup>mock-transfected</sup> or sEV<sup>PUNISHER-downregulated</sup> treatment by PCR array. The five genes with a >2-fold change are labeled and listed. (C) Differentially expressed genes in the PCR array with their

(legend continued on next page)

study, we sought to elucidate the role of sEV-incorporated lncRNA *PUNISHER* in CAD patients and to understand their impact on the regulation of vascular integrity.

We utilized a PCR-based human lncRNA array to investigate differentially regulated lncRNAs in sEVs that were derived from plasma of patients with CAD or NCAD. This array revealed a number of lncRNAs that were highly upregulated in CAD patients. Based on the results of our array as well as the current literature, we investigated the plasma-sEV levels of four atherosclerosis-related lncRNAs: *PUNISHER*, *GASS*, *H19*, and *MALATI*. Among them, the largest difference between NCAD and stable CAD patients was seen for *PUNISHER*. The majority of lncRNA studies in CAD have focused on whole circulating lncRNAs (in plasma, serum, or whole blood) rather than EV-incorporated circulating lncRNAs.<sup>7,73</sup> Notably, a recent study demonstrated that the lncRNA CoroMarker, which is considered to be a novel biomarker for CAD, is primarily found in circulating EVs.<sup>74</sup> Our current findings provide further in-depth insights into the regulation of the EV-incorporated lncRNA *PUNISHER* under the clinical and experimental conditions of vascular diseases.

In analogy to our clinical findings, the *in vitro* experiments revealed that *PUNISHER* levels increased following stimulation with oxLDL and TNF- $\alpha$  in ECs and EC-derived sEVs, which indicates a response to two independent pro-atherogenic stimuli. Recent studies indicated that lncRNAs act as key players in atherosclerosis-related pathological conditions, e.g., EC functional dysregulation and vascularization.<sup>75,76</sup> *PUNISHER* is known to be required for angiogenesis.<sup>41</sup>

It has been shown previously that ncRNAs are selectively packaged by cells into the corresponding EVs.<sup>60</sup> Previous studies have revealed RBPs, including the hnRNP family, which can facilitate selective packaging of ncRNAs into EV (e.g., hnRNPA2B1, Y box binding protein 1 [Y-BOX1], SYNCRIP, and Argonaute protein 2 [AGO2]).<sup>52,77</sup> In the present study, we discovered that the multifunctional RBP hnRNPK interacts with *PUNISHER* and facilitates its loading into sEVs, providing novel mechanistic insights into the cellular sorting and packaging of lncRNAs into sEVs. Finally, in recipient cells, *PUNISHER* regulates transcription and expression levels of the pro-angiogenic gene *VEGFA*.

The horizontal transfer of sEV cargoes represents an effective means of biological signaling between parent and recipient cells in diverse settings.<sup>78</sup> Within this context, the exosome-transmitted lncRNA *ARSR* has been shown to ameliorate drug resistance in cancer.<sup>53</sup> Furthermore, the cholangiocyte-derived exosomal lncRNA *H19* was reported to accelerate cholestatic liver injury.<sup>79,80</sup>

Although studies have revealed that sEVs deliver lncRNAs in oncologic or other diseases, a role for sEV-mediated lncRNA transfer in

the regulation of vascular function has not been previously shown. Our data show, for the first time, that sEV-mediated transfer of a vascular lncRNA, namely *PUNISHER*, into target ECs promotes an angiogenic response. sEV-incorporated *PUNISHER* downregulates mRNA levels of the pro-angiogenic protein *VEGFA* in recipient ECs. The role of angiogenesis in CAD is thought to have a dual effect.<sup>41,76,78</sup> In ischemic heart disease (IHD), pro-angiogenic factors could accelerate neointima formation and promote microvascular network growth, thus contributing to the improvement of myocardial reperfusion.<sup>76</sup> In the adult organism, angiogenesis only takes place during the female menstrual cycle and during wound healing. Under pathological conditions, angiogenesis is involved in tumor development, diabetic retinopathy, and IHD, which can be a consequence of atherosclerosis, a sequelae of CAD. In atherosclerosis, angiogenesis facilitates the growth of atherosclerotic lesions; angiogenesis within plaques plays a crucial role in plaque destabilization and rupture.<sup>71</sup> In our study, we found that the pro-angiogenic lncRNA *PUNISHER* is upregulated in the plasma sEVs of stable CAD patients. *In vitro*, *PUNISHER* was found to regulate the angiogenic function of recipient ECs via the transport of *PUNISHER*-incorporated sEVs. This result indicates that the increased level of *PUNISHER* in sEVs might be triggered by ischemia and can ameliorate myocardial ischemia in CAD patients by promoting neovascularization. However, in patients with stable plaques, the participation of *PUNISHER* in intraplaque angiogenesis and the potential for a resulting plaque rupture should also be considered. However, these findings are important to understand the mechanism of angiogenesis in CAD as well as other pathological settings (cancer), hinting that future investigations are required to provide deeper explanations for the clinical significance. Our results demonstrate that sEV-incorporated *PUNISHER* expression is significantly higher in CAD patients when compared with NCAD patients. *In vitro*, we found that functional *PUNISHER* can be transferred to target ECs, which promotes an angiogenic response. Pharmacological inhibition of *PUNISHER* expression is accompanied by an impairment of the angiogenic response and a decrease in cell proliferation.

Mechanistically speaking, the binding partner of *PUNISHER*, hnRNPK, is a multifunctional RBP that regulates the cytoplasmic fate of mRNAs by regulating their stability or translation, and it is known to bind a number of mRNAs, including *VEGFA*.<sup>63,64</sup> We found that *PUNISHER* binds to the RBP hnRNPK, which changes the binding of hnRNPK to its cognate mRNA, *VEGFA*, by binding to its 3' UTR, as previously reported.<sup>63,64</sup> The stability of the *VEGFA* mRNA transcript is downregulated in *PUNISHER*-silenced cells in comparison to siScr-treated cells, suggesting that *PUNISHER* may also regulate the transcription of *VEGFA*. When we further analyzed the protein stability of *VEGFA* in these cells, it was confirmed that *PUNISHER* also regulates the stability of *VEGFA* protein, thereby controlling the angiogenic function of ECs.

---

respective fold change in donor and recipient ECs. (D) Venn diagram showing common genes in both assays. *VEGFA* was the only gene shared by the two PCR arrays (fold change = 2.0). (E and F) Individual qRT-PCR validation of *VEGFA*, which was downregulated in the angiogenesis arrays. The downregulation of the *VEGFA* gene from the array was confirmed by individual qRT-PCR in ECs. *VEGFA* RNA expression was analyzed in ECs by qRT-PCR (\*p < 0.5, n = 3, by Student's t test). (G and H) *VEGFA* protein levels in donor or recipient ECs were quantified from western blotting.

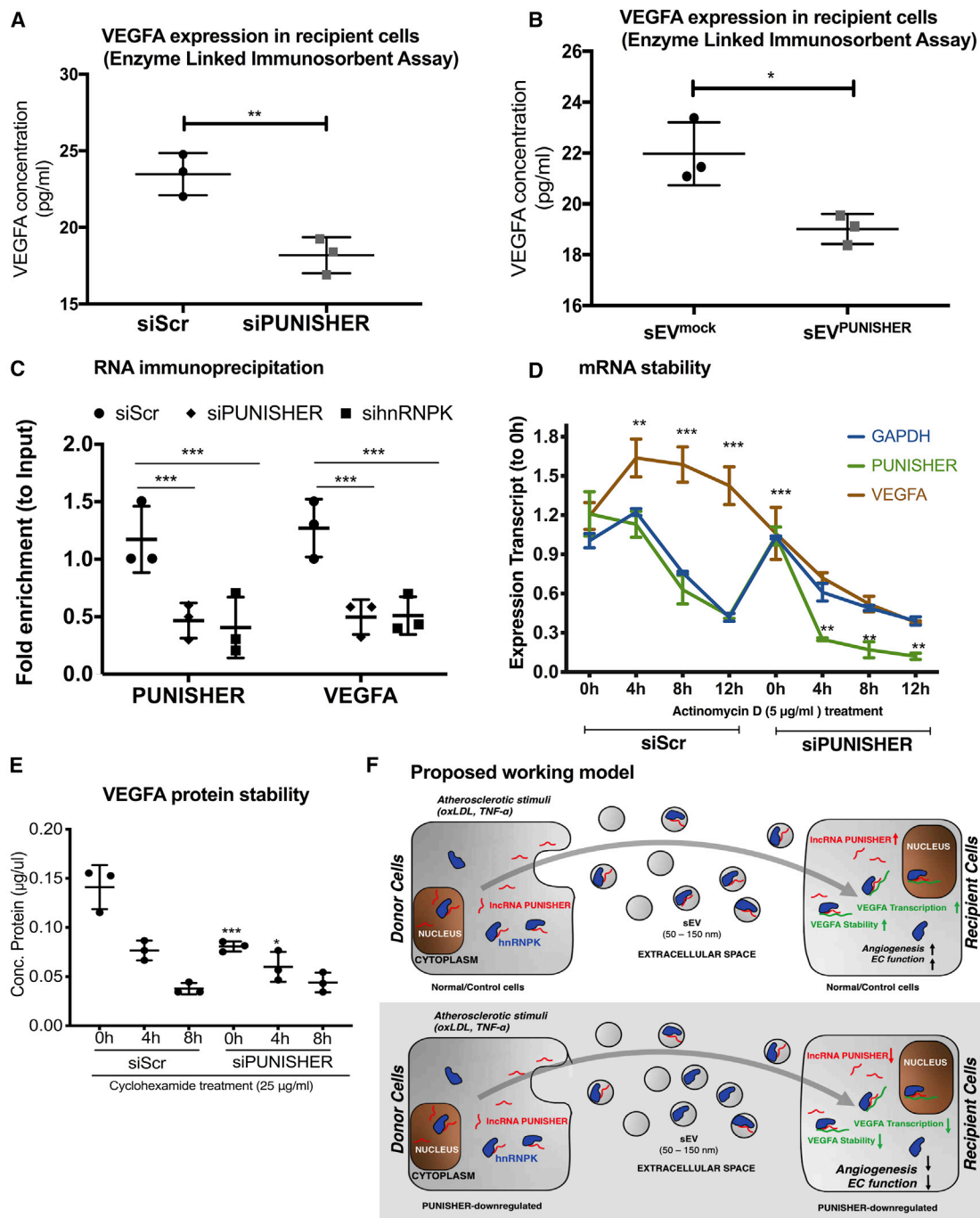


**Figure 7. PUNISHER is crucial for VEGFA regulation**

(A and B) ECs were transfected with *PUNISHER* siRNA or control siRNA. Secreted VEGFA protein levels were quantified via enzyme-linked immunosorbent assay (ELISA) from donor-EC culture media and recipient cells treated with sEVs after siScr and siPUNISHER treatment (\*\**p* < 0.01, *n* = 6 by Student's *t* test). (C) Cross-linked RIP experiments followed by qRT-PCR quantification to confirm consequence of *PUNISHER* or hnRNPk silencing regulate binding of *VEGFA* mRNA to RBP. This reciprocal binding of *PUNISHER* to hnRNPk in human ECs is important to control VEGFA protein synthesis. From RIP experiments, binding of hnRNPk was quantified in comparison to IgG (negative control) upon siRNA treatment. Quantification was performed by normalizing the values with the inputs (10%). Data represent the mean ± SD (\*\**p* < 0.001, *n* ≥ 4, by Student's *t* test). (D) The stability of *PUNISHER* and *VEGFA* RNA by using actinomycin D (Ac-D) treatment (5 μg/mL for different time points) upon siRNA knockdown of *PUNISHER* or a scrambled control. The expression of mRNAs was analyzed by qRT-PCR in donor cells after siRNA treatment (\**p* < 0.5, *n* = 6, by Student's *t* test). (E) Stability of VEGFA protein was analyzed at different time points by using cells treated with cycloheximide (CHX) to a final concentration of 25 μg/mL upon siRNA treatment against

(legend continued on next page)

Most importantly, when RIP-qPCR was performed with primer pairs that target the 3' UTR (which contains the VEGFA-binding regions), significantly less binding of hnRNPK to VEGFA was recorded in *PUNISHER*- or hnRNPK-silenced cells (Figures 3D-3F). This result suggests that the interaction between *PUNISHER* and hnRNPK is indispensable for the efficient binding of VEGFA. When hnRNPK is knocked down, it is possible that the expression of VEGFA is reduced, which could be facilitated by the lncRNA *PUNISHER*, as we observed more binding on normally grown ECs than *PUNISHER*-silenced ECs and confirmed that *PUNISHER* is important for EC function. To our knowledge, this is the first time that clinical and experimental atherosclerotic conditions have been shown to promote the packaging of functional *PUNISHER* into sEVs, thus inducing an angiogenic phenotype in the recipient ECs. Taking all of the above-mentioned data together, we have confirmed that *PUNISHER* silencing lowers the stability of the basal level of VEGFA, which is regulated via the hnRNPK-*PUNISHER* interaction, thereby regulating the angiogenic function of ECs.

However, our study has some limitations, namely, the patient samples were all collected at the University of Bonn, Germany; thus, the patient-derived data presented are limited to the Caucasian race. In addition, we generated sEV<sup>*PUNISHER* downregulated</sup> through the efficient knockdown of *PUNISHER* in sEV-producing parent ECs. Although the expression levels of the other four lncRNAs analyzed were not affected in these sEVs, as confirmed by qRT-PCR, it is technically challenging to completely exclude that there was a change to any of the other biological contents of the sEVs.

In conclusion, our findings offer the following insights into the role of lncRNAs as intercellular signaling molecules. (1) We show for the first time that sEV-incorporated lncRNAs are regulated under the clinical and experimental conditions of atherosclerosis. (2) The lncRNA *PUNISHER* is primarily incorporated within sEVs, and this packaging happens in an hnRNPK-dependent manner. (3) *PUNISHER* is shuttled between cells via sEVs to increase the angiogenic response by increasing VEGFA expression in the recipient ECs. In summary, our study has revealed that sEV-incorporated *PUNISHER* has a dual function as both a biomarker and effector of vascular integrity.

## MATERIALS AND METHODS

### Study subjects

The study enrolled patients presenting in our outpatient and emergency departments between August 2012 and July 2013. All clinical samples were collected with the appropriate informed consent from patients in the department. Ethical approval was granted from the Ethics Committee of the University of Bonn (approval number [no.] 05/12) and followed the principles outlined in the Declaration of Hel-

sinki. Based on the data from the clinical presentation, laboratory parameters, and coronary angiography, patients were classified into two groups: angiographic exclusion of obstructive CAD (<50% stenosis of a major coronary artery, named as NCAD) and stable CAD. Further exclusion criteria for our study were as follows: (1) chronic inflammatory disease, (2) acute kidney or liver disease, (3) malignant disease, and (4) the patients who declined to participate.

### Preparation of blood samples

Blood samples were collected under sterile conditions from the cubital vein and buffered by using sodium citrate. In order to generate platelet-depleted plasma samples, blood was first centrifuged at  $1,500 \times g$  for 15 min; the supernatant was then centrifuged at  $13,000 \times g$  for 20 min. Platelet-deficient plasma samples were stored at  $-80^{\circ}\text{C}$ , and repeated freeze-thaw cycles were avoided until the sEVs were isolated.

### Cell culture

HCAECs (PromoCell) were cultured in EC growth media with endothelial growth media supplement mix (PromoCell; #C-39225) under standard cell culture conditions ( $37^{\circ}\text{C}$ , 5%  $\text{CO}_2$ ) in a standard humidified incubator. Cells from passages 5–7 were used. At least three biologically independent batches of cells were studied in each experiment.

For the isolation of sEVs, HCAECs were cultured as previously described.<sup>69,81,82</sup> Briefly, confluent cells were first washed 3 times with conditioned medium and then starved in conditioned medium (basal medium without growth media supplements; PromoCell; #C-22020) for 24 h. After starvation, the supernatant was collected for sEV isolation.

### sEV generation

A previously described ultracentrifugation method was used for the isolation of sEVs.<sup>83</sup> Briefly, 2.5 mL plasma (following 1:4 dilution) or 8 mL conditioned cell culture medium (collected from  $8 \times 10^6$  donor ECs) was first centrifuged at  $3,000 \times g$ ,  $4^{\circ}\text{C}$  for 15 min, to deplete the cell debris; IEVs were removed by centrifugation at  $20,000 \times g$ ,  $4^{\circ}\text{C}$  for 40 min, as previously described.<sup>69,81,82</sup> Then the supernatant was centrifuged at  $100,000 \times g$ ,  $4^{\circ}\text{C}$  for 90 min, in a Beckman Coulter Optima LE-80K ultracentrifuge with a type SW 41Ti rotor (K-factor: 256.6) to pellet the sEVs. The pellet was resuspended in 8 mL sterile ice-cold PBS followed by re-centrifugation at  $100,000 \times g$ ,  $4^{\circ}\text{C}$  for 90 min, to purify the sEVs.<sup>83,84</sup> The sEV pellet was resuspended in sterile  $1 \times \text{PBS}$  and used immediately.

### RNA isolation and qRT-PCR

Total RNA was isolated by using the miRNeasy Mini Kit (QIAGEN; #217004) extraction method according to the instructions of the manufacturer. RNA was diluted in UltraPure DNase/RNase-Free

---

*PUNISHER* or a scrambled siRNA control by western blotting. Anti-histone-3 (H3) was used as a loading control. (F) Schematic representation of the working model of sEV-incorporated *PUNISHER* transport. Atherosclerotic stimuli increase the level of *PUNISHER* both in donor cells and incorporated into sEVs. hnRNPK regulates the loading of *PUNISHER* into sEVs from ECs. sEV-mediated transfer of *PUNISHER* regulates the migration, proliferation, sprouting, and network formation of recipient ECs by controlling VEGFA stability.

Distilled Water (Invitrogen). RNA concentration and purity (absorbance at 260/280 nm [A260/A280] and A260/A230) were quantified using a Nanodrop spectrophotometer (Table S1). 2 µg RNA (HCAEC) or 300 µg RNA (sEV) was reverse transcribed by using an Omniscript RT kit (QIAGEN; #205113), according to the manufacturer's protocol. In addition, the purity and integrity of RNA isolated from patient plasma with CAD (n = 6) and NCAD (n = 6) were assessed by using an Agilent Bio-analyzer with the Agilent RNA 6000 Nano Kit (Agilent Technologies; #5067-1511). 5 ng of cDNA template was used for the quantification by using TaqMan assays (Thermo Fisher Scientific) on a 7500 HT Real-Time PCR machine (Applied Biosystems). The intra-/inter-assay variability of *PUNISHER* detection in plasma sEVs was <5%.

The expression profile of *PUNISHER* was checked by using human tissue samples, and purified RNA was purchased from commercial vendors as follows: Human Total RNA Master Panel II (Clontech; #636643; lot no. 1202050A); human heart (Amsbio; #R1234122-50; lot no. A804058).

#### Human lncRNA PCR array

The expression of 372 lncRNAs with known biological functions or disease associations as well as well-characterized functional lncRNAs was quantified via an Arraystar Human Functional lncRNA Array (Arraystar, Rockville, MD, USA). The samples were prepared based on the manufacturer's standard protocols, with only minor modification. Briefly, total RNAs from sEVs isolated from the plasma of NCAD and CAD patients were isolated by using a miRNeasy kit (QIAGEN, Hilden, Germany), and 1.5 µg RNA was reverse transcribed by using an rt-STAR First-strand cDNA synthesis kit (Arraystar; catalog [cat.] #AS-FS-001), according to the manufacturer's protocol. Six human housekeeping genes, *ACTB*, *B2M*, *Gusb*, *Hsp90ab1*, glyceraldehyde 3-phosphate dehydrogenase (*GAPDH*), and 18S rRNA, were included as the internal qPCR normalization references.

In-plate genomic DNA controls (GDCs) were used on the array plate to confirm the quality of the cDNA template for qRT-PCR analysis. Quantification of lncRNAs was performed by using the 7900HT Fast Real-Time PCR System. Data were normalized by using an in-plate housekeeping gene, *GAPDH*. Data analysis was performed with SDS 2.4 data analysis software (Applied Biosystems, USA), and further analyses were conducted with an RQ Manager 1.2.1 data analysis tool.

#### Atherosclerotic stimuli treatment *in vitro*

Confluent HCAECs were treated with 25 µg/mL or 50 µg/mL oxLDL (Alfa Aesar; #J65591) for 24 h. Similarly, HCAECs were treated by using different TNF-α (R&D Systems; #210-TA-020) concentrations (10 ng/mL, 20 ng/mL, or 50 ng/mL). Then the cells were subjected to basal media for 24 h to generate the corresponding sEVs.

#### Endothelial sEV internalization into recipient EC

HCAECs were stained with PKH67 (Sigma-Aldrich; #MIDI67), according to the manufacturer's instructions. PKH67-labeled sEVs

were washed twice with PBS.  $2 \times 10^5$  recipient ECs were co-incubated with PKH67-labeled sEVs (1.5 µg sEV, equivalent to sEVs collected from  $8 \times 10^6$  donor ECs) for 0, 0.5, 6, or 24 h. Nuclei were counterstained with 4',6-diamidino-2-phenylindole (DAPI; Vector Laboratories; #H-1200). A Zeiss Axiovert 200M microscope and ZEN 2.3 Pro software was used to visualize the uptake of sEVs into the recipient HCAECs.

#### Co-incubation of endothelial sEVs and recipient ECs

$2 \times 10^5$  recipient ECs were co-incubated with 1.5 µg sEV (equivalent to sEV collected from  $8 \times 10^6$  donor ECs) or PBS for 24 h. Then the ECs were washed three times with PBS. Total RNA was isolated from all EC samples for qRT-PCR analysis.

#### Knockdown experiments in ECs

Transient siRNA transfection (10 nM final concentrations) of semi-confluent HCAECs (50%–60% confluent) was carried out for 48 h using the HiPerFect reagent (QIAGEN), according to the manufacturer's protocol.

#### RIP

A Magna RIP Kit (Millipore; #17-700) was used according to the manufacturer's protocol. For each RIP reaction, 100 µL of the cellular pellet was fixed with 1% formaldehyde in PBS at room temperature for 10 min. For one RIP reaction (i.e., one IP using one antibody), 100 µL of cell lysate or  $\sim 5.0 \times 10^6$  cells were used. The cross-linking reaction was stopped by adding 590 µL of 2.5 M glycine. Fixed cells were subsequently harvested and resuspended in RIP lysis buffer supplemented with protease/RNase inhibitors. The lysates were obtained using a Dounce homogenizer on ice (10 passes to release the nuclei) followed by incubation on ice for 15 min. An equal volume of RIP lysis buffer was added to the cellular pellet. From the solution, 10 µL (10%) of the lysates was removed and stored as an "input," as recommended by the manufacturer. For each RIP reaction, 100 µL of lysate was mixed with 5 µg of mouse anti-immunoglobulin G (IgG; negative control provided with the kit) or anti-hnRNPK antibody (Abcam) that had been previously conjugated with protein A/G magnetic beads (provided with the kit). After incubating overnight at 4°C, the RNA-protein precipitate was extensively washed with RIP Wash Buffer (provided with the kit). The cross-linking was reversed by incubation with proteinase K. The RIP was purified through phenol/chloroform/isoamyl alcohol (125:24:25) isolation. The purified RIP was treated with DNase I (Thermo Fisher Scientific; #AM2239) and reverse transcribed using SuperScript VILO Master Mix (Thermo Fisher Scientific; #11755050).

#### hnRNP-K IP

IP was performed using the Dynabeads Protein G Immunoprecipitation Kit (Invitrogen). For one sample, with respective controls,  $7.2 \times 10^7$  HCAECs were lysed in Nonidet P-40 (NP-40) cell lysis buffer (Invitrogen) and centrifuged at  $13,000 \times g$  for 20 min at 4°C. The lysate was pre-cleared with 50 µL Dynabeads per 1,000 µL lysate for 60 min at 4°C. After coupling of 10 µg of monoclonal mouse anti-hnRNP-K antibody (Abcam) or mouse IgG1 kappa monoclonal isotype control

antibody (Abcam) to 50  $\mu$ L Protein G Dynabeads for 1 h at room temperature, 1,000  $\mu$ L of lysate was incubated with the antibody-coupled beads for 16 h at 4°C. Samples were washed extensively, and the RNA was eluted twice with 20  $\mu$ L of the provided elution buffer. Protein samples were isolated according to the recommended protocol of the manufacturer.

#### Western blotting

As a control for the sEVs isolated from plasma in immunoblotting, whole plasma was used, whereas for endothelial sEVs, cell lysate and conditioned media (growth media without growth media supplements; PromoCell; #C-22020) were used as the control. Cells were homogenized in radioimmunoprecipitation assay buffer (RIPA) buffer (Sigma-Aldrich; #R0278) including a protease inhibitor cocktail (Roche; #11 873 580 001) on ice. The protein concentration of the corresponding samples was measured by a Lowry protein assay (BioRad; #500-0116). An equal amount of protein (20  $\mu$ g) for sEVs, plasma, or cells was loaded onto 4%–15% precast polyacrylamide gels (BioRad; #456-1084). Then the gel was transferred to a polyvinylidene fluoride (PVDF) membrane (Thermo Fisher Scientific; #88585), followed by blocking in 5% BSA in Tris-buffered saline with 0.1% Tween 20 (TBST). The blots were incubated with the appropriate primary antibodies, and detection was performed by using the appropriate secondary antibody. The membranes were imaged using chemiluminescence via an Enhanced Chemiluminescence (ECL) Detection Kit (GE Healthcare; #RPN2232).

#### Electron microscopy

For TEM, sEVs from plasma or from ECs were pelleted by centrifugation, fixed in 1.25% glutaraldehyde in 0.1 M cacodylate buffer overnight, dehydrated with ethanol and propylene oxide, and embedded in Epon 812 (Serva), also overnight. After double-contrast staining with uranyl acetate and an aqueous lead solution, images were taken with a CM 10 electron microscope (Philips).

#### Vesicle-RNA degradation assay

For the degradation assay, 45  $\mu$ L proteinase K (Thermo Fisher Scientific; #25530049) was used for protein digestion, with or without the presence of 45  $\mu$ L Triton X-100 (Sigma-Aldrich; #T8787) for 30 min at 37°C. The samples were then treated with 5  $\mu$ L RNase A (Thermo Fisher Scientific; #AM2271) for 20 min at 37°C. The untreated group was used as a normal control. Total RNA was isolated from all sEV samples for qRT-PCR analysis.

#### Manipulated sEV generation and recipient EC treatment

To generate sEV<sup>PUNISHER downregulated</sup> and sEV<sup>mock transfected</sup>, HCAECs were transfected with *PUNISHER* siRNA or control siRNA using HiPerFect for 48 h and exposed to conditioned media for 24 h to generate the modified sEVs.  $2 \times 10^5$  recipient HCAECs were co-incubated with the same amount (1.5  $\mu$ g) of sEVs, sEV<sup>PUNISHER downregulated</sup>, or sEV<sup>mock transfected</sup> and PBS for 24 h. ECs were washed three times with PBS. The ECs from different groups were then used for the following functional assays.

#### mRNA and protein stability

A total of 20,000 HUVECs were plated into a 6-well plate (Greiner bio-one; cat. #657160) prior to incubation for 24 h under optimal cell-growth conditions (5% CO<sub>2</sub> and 37°C in an incubator). Afterward, the growth medium was replenished, followed by two times more after incubation. Cells were induced with 5  $\mu$ g/mL actinomycin D (Sigma-Aldrich; product no. A9415) added to the culture medium, followed by a time-wise collection of RNA with TRIzol (Invitrogen) at 1, 2, 4, 6, 12, and 24 h. For CHX, 500 mg CHX powder was dissolved and homogenized in 5 mL sterile DMSO to prepare 10 mg/mL stock solution. A similar number of cells were treated with CHX to a final concentration of 25  $\mu$ g/mL. Protein and RNA from untreated cells at 0 h were also collected as a control. For cDNA preparation, 1  $\mu$ g RNA was treated with DNase I and reverse transcribed by using Super-Script VILO Master Mix (Invitrogen; cat. no. 11755050) prior to cDNA preparation, which was finally diluted to 1 ng/ $\mu$ L for qRT-PCR analysis.

#### In vitro network formation assay

After thawing overnight at 4°C, 250  $\mu$ L Growth Factor Reduced (GFR) Matrigel (Thermo Fisher Scientific; #A1413202) was placed into each well of cold 24-well plates using cold pipette tips, and the plates were then placed at room temperature for 30 min.  $4 \times 10^4$  HCAECs were placed in each of the Matrigel-coated wells and incubated for 24 h under standard cell culture conditions (37°C, 5% CO<sub>2</sub>). Wells containing PBS were used as controls. To analyze the dose-dependent rescue, three different exogenous VEGFA concentrations: 0 pg/mL, 500 pg/mL, and 5,000 pg/mL were used. Network formation was quantified by measuring the number of branches, number of loops, and total length of the tube. Digital images of microtiter well sections were obtained by using a Zeiss Axiovert 200M microscope and ZEN 2.3 Pro software. Data were analyzed with ImageJ image analysis software (NIH, USA).

#### Human VEGFA ELISAs

Protein levels of the human VEGFA (Abcam; #ab119566) were monitored in the supernatant of EC cultures by using commercial ELISAs, following the manufacturer's instructions. Each sample was assayed with two replicates (duplicates), and the absorbance was measured by a spectrophotometer (TECAN; Infinite M200 Microplate reader) at 450 nm as the primary wavelength. Curve fitting and data analysis were accomplished by CurveExpert Pro software (Hyams Development, USA).

#### RT<sup>2</sup> Profiler angiogenesis PCR array gene expression

Total RNA was isolated out of HCAECs by using an RNeasy Mini Kit (QIAGEN; #74104), according to the manufacturer's instructions. Then, 1  $\mu$ g of the total RNA was reverse transcribed by using an RT<sup>2</sup> First Strand Kit (QIAGEN), according to the manufacturer's protocol. RT<sup>2</sup> Profiler PCR Array Analysis (QIAGEN; #PAHS-024Z) was performed to measure the expression of 84 key genes involved in modulating the biological processes of angiogenesis. PCR was carried out on an Applied Biosystems 7500 HT Real-Time PCR machine.

Detailed data analysis was performed by and exported from the QIAGEN GeneGlobe Data Analysis Center.

#### Data availability

The raw proteomic data were recently published by our group.<sup>54</sup> The Human Functional lncRNA Array and *in silico* target prediction data have been provided in [Tables S5](#) and [S6](#). All further data that support the findings of this manuscript are available on request from the corresponding authors.

#### Statistical analysis

Normally distributed continuous variables were presented as the mean  $\pm$  SD. Continuous variables were tested for normal distribution with the use of the Kolmogorov-Smirnov test. Categorical variables are given as frequencies and percentages. For continuous variables, a Student's *t* test or Mann-Whitney *U* test was used for the comparison between two groups. For the comparison of >2 groups, the one-way ANOVA with Bonferroni correction for multiple comparisons test was used. The chi-square test was used for categorical data that resulted from classifying objects. Binary logistic regression was applied to identify factors that were independently associated with *PUNISHER*. All tests were two sided, and statistical significance was assumed when the null hypothesis could be rejected at  $p < 0.05$ . Statistical analysis was performed with IBM SPSS Statistics version 20 (IBM, USA) and GraphPad Prism 7 (GraphPad, USA).

An extended [Supplemental materials and methods](#) can be found in the online [Supplemental information](#).

#### SUPPLEMENTAL INFORMATION

Supplemental information can be found online at <https://doi.org/10.1016/j.omtn.2021.05.023>.

#### ACKNOWLEDGMENTS

We thank Ms. Anna Flender, Ms. Paula Levermann, and Ms. Sarah Arahouan for their excellent technical assistance. We also thank Dr. Meghan Lucas for her critical reading of the manuscript. We thank the Core Facility Mass Spectrometry at the Institute of Biochemistry and Molecular Biology, Medical Faculty, University of Bonn, for performing mass spectrometry analysis. The authors also acknowledge cooperation with the MPI, Dortmund, for support with electron microscopy. M.R.H. is funded by the German Society of Cardiology (DGK). This study was supported by the German Research Foundation (DFG) under grants WE 4139/8-1 and JA 2351/2-1. The study was further supported by a translational grant from the Corona Foundation and Deutsche Forschungsgemeinschaft (German Research Foundation) project ID 397484323-TRR 259 (project B04).

#### AUTHOR CONTRIBUTIONS

M.R.H. and F.J. supervised and conceptualized the study and prepared the manuscript. Q.L., M.R.H., Y.Y., A.Z., K.M., and P.G. performed the *in vitro/in vivo* experiments. S.U., E.L., N.W., G.N., and F.J. contributed intellectually to the development and funding of the project. All authors have read and approved the final manuscript.

#### DECLARATION OF INTERESTS

The authors have no competing interests.

#### REFERENCES

- Boulanger, C.M., Loyer, X., Rautou, P.-E., and Amabile, N. (2017). Extracellular vesicles in coronary artery disease. *Nat. Rev. Cardiol.* *14*, 259–272.
- Ray, D.M., Spinelli, S.L., Pollock, S.J., Murant, T.I., O'Brien, J.J., Blumberg, N., Francis, C.W., Taubman, M.B., and Phipps, R.P. (2008). Peroxisome proliferator-activated receptor  $\gamma$  and retinoid X receptor transcription factors are released from activated human platelets and shed in microparticles. *Thromb. Haemost.* *99*, 86–95.
- Brill, A., Dashevsky, O., Rivo, J., Gozal, Y., and Varon, D. (2005). Platelet-derived microparticles induce angiogenesis and stimulate post-ischemic revascularization. *Cardiovasc. Res.* *67*, 30–38.
- Owens, A.P., 3rd, and Mackman, N. (2011). Microparticles in hemostasis and thrombosis. *Circ. Res.* *108*, 1284–1297.
- Yang, Y., Cai, Y., Wu, G., Chen, X., Liu, Y., Wang, X., Yu, J., Li, C., Chen, X., Jose, P.A., et al. (2015). Plasma long non-coding RNA, CoroMarker, a novel biomarker for diagnosis of coronary artery disease. *Clin. Sci. (Lond.)* *129*, 675–685.
- Fiedler, J., Baker, A.H., Dimmeler, S., Heymans, S., Mayr, M., and Thum, T. (2018). Non-coding RNAs in vascular disease - from basic science to clinical applications: scientific update from the Working Group of Myocardial Function of the European Society of Cardiology. *Cardiovasc. Res.* *114*, 1281–1286.
- Viereck, J., and Thum, T. (2017). Circulating noncoding RNAs as biomarkers of cardiovascular disease and injury. *Circ. Res.* *120*, 381–399.
- Helsmoortel, H., Everaert, C., Lumen, N., Ost, P., and Vandesompele, J. (2018). Detecting long non-coding RNA biomarkers in prostate cancer liquid biopsies: Hope or hope? *Noncoding RNA Res.* *3*, 64–74.
- Born, L.J., Harmon, J.W., and Jay, S.M. (2020). Therapeutic potential of extracellular vesicle-associated long noncoding RNA. *Bioeng. Transl. Med.* *5*, e10172.
- Zhang, Y., Zhang, L., Wang, Y., Ding, H., Xue, S., Qi, H., and Li, P. (2019). MicroRNAs or long noncoding RNAs in diagnosis and prognosis of coronary artery disease. *Aging Dis.* *10*, 353–366.
- Arroyo, J.D., Chevillet, J.R., Kroh, E.M., Ruf, I.K., Pritchard, C.C., Gibson, D.F., Mitchell, P.S., Bennett, C.F., Pogosova-Agadjanyan, E.L., Stirewalt, D.L., et al. (2011). Argonaute2 complexes carry a population of circulating microRNAs independent of vesicles in human plasma. *Proc. Natl. Acad. Sci. USA* *108*, 5003–5008.
- Tabet, F., Vickers, K.C., Cuesta Torres, L.F., Wiese, C.B., Shoucri, B.M., Lambert, G., Catherinet, C., Prado-Lourenco, L., Levin, M.G., Thacker, S., et al. (2014). HDL-transferred microRNA-223 regulates ICAM-1 expression in endothelial cells. *Nat. Commun.* *5*, 3292.
- Tkach, M., and Théry, C. (2016). Communication by extracellular vesicles: where we are and where we need to go. *Cell* *164*, 1226–1232.
- He, L., and Hannon, G.J. (2004). MicroRNAs: small RNAs with a big role in gene regulation. *Nat. Rev. Genet.* *5*, 522–531.
- Kung, J.T., Colognori, D., and Lee, J.T. (2013). Long noncoding RNAs: past, present, and future. *Genetics* *193*, 651–669.
- Mercer, T.R., Dinger, M.E., and Mattick, J.S. (2009). Long non-coding RNAs: insights into functions. *Nat. Rev. Genet.* *10*, 155–159.
- Wilusz, J.E., Sunwoo, H., and Spector, D.L. (2009). Long noncoding RNAs: functional surprises from the RNA world. *Genes Dev.* *23*, 1494–1504.
- Bayoumi, A.S., Sayed, A., Broskova, Z., Teoh, J.-P., Wilson, J., Su, H., Tang, Y.-L., and Kim, I.M. (2016). Crosstalk between long noncoding RNAs and microRNAs in health and disease. *Int. J. Mol. Sci.* *17*, 356.
- Liu, Y., Li, Q., Hosen, M.R., Zietzer, A., Flender, A., Levermann, P., Schmitz, T., Frühwald, D., Goody, P., Nickenig, G., et al. (2019). Atherosclerotic conditions promote the packaging of functional MicroRNA-92a-3p into endothelial microvesicles. *Circ. Res.* *124*, 575–587.
- Jansen, F., Yang, X., Hoelscher, M., Cattelan, A., Schmitz, T., Proebsting, S., Wenzel, D., Vosen, S., Franklin, B.S., Fleischmann, B.K., et al. (2013). Endothelial microparticle-mediated transfer of MicroRNA-126 promotes vascular endothelial cell repair



- via SPRED1 and is abrogated in glucose-damaged endothelial microparticles. *Circulation* 128, 2026–2038.
21. Loyer, X., Vion, A.-C., Tedgui, A., and Boulanger, C.M. (2014). Microvesicles as cell-cell messengers in cardiovascular diseases. *Circ. Res.* 114, 345–353.
  22. De Rosa, S., Curcio, A., and Indolfi, C. (2014). Emerging role of microRNAs in cardiovascular diseases. *Circ. J.* 78, 567–575.
  23. Thum, T., and Mayr, M. (2012). Review focus on the role of microRNA in cardiovascular biology and disease. *Cardiovasc. Res.* 93, 543–544.
  24. Fichtlscherer, S., De Rosa, S., Fox, H., Schwietz, T., Fischer, A., Liebetrau, C., Weber, M., Hamm, C.W., Röxe, T., Müller-Ardogan, M., et al. (2010). Circulating microRNAs in patients with coronary artery disease. *Circ. Res.* 107, 677–684.
  25. Hinger, S.A., Cha, D.J., Franklin, J.L., Higginbotham, J.N., Dou, Y., Ping, J., Shu, L., Prasad, N., Levy, S., Zhang, B., et al. (2018). Diverse long RNAs are differentially sorted into extracellular vesicles secreted by colorectal cancer cells. *Cell Rep.* 25, 715–725.e4.
  26. Kumarswamy, R., Bauters, C., Volkman, I., Maury, F., Fetisch, J., Holzmann, A., Lemesle, G., de Groote, P., Pinet, F., and Thum, T. (2014). Circulating long noncoding RNA, LIPCAR, predicts survival in patients with heart failure. *Circ. Res.* 114, 1569–1575.
  27. Uchida, S., and Dimmeler, S. (2015). Long noncoding RNAs in cardiovascular diseases. *Circ. Res.* 116, 737–750.
  28. Skroblin, P., and Mayr, M. (2014). “Going long”: long non-coding RNAs as biomarkers. *Circ. Res.* 115, 607–609.
  29. Jimenez, L., Yu, H., McKenzie, A.J., Franklin, J.L., Patton, J.G., Liu, Q., and Weaver, A.M. (2019). Quantitative Proteomic Analysis of Small and Large Extracellular Vesicles (EVs) Reveals Enrichment of Adhesion Proteins in Small EVs. *J. Proteome Res.* 18, 947–959.
  30. Jansen, F., Li, Q., Pfeifer, A., and Werner, N. (2017). Endothelial- and Immune Cell-Derived Extracellular Vesicles in the Regulation of Cardiovascular Health and Disease. *JACC Basic Transl. Sci.* 2, 790–807.
  31. Li, Q., Shao, Y., Zhang, X., Zheng, T., Miao, M., Qin, L., Wang, B., Ye, G., Xiao, B., and Guo, J. (2015). Plasma long noncoding RNA protected by exosomes as a potential stable biomarker for gastric cancer. *Tumour Biol.* 36, 2007–2012.
  32. Naderi-Meshkin, H., Lai, X., Amirkhah, R., Vera, J., Rasko, J.E.J., and Schmitz, U. (2019). Exosomal lncRNAs and cancer: connecting the missing links. *Bioinformatics* 35, 352–360.
  33. Dragomir, M., Chen, B., and Calin, G.A. (2018). Exosomal lncRNAs as new players in cell-to-cell communication. *Transl. Cancer Res.* 7 (Suppl 2), S243–S252.
  34. Qi, P., Zhou, X.Y., and Du, X. (2016). Circulating long non-coding RNAs in cancer: current status and future perspectives. *Mol. Cancer* 15, 39.
  35. Théry, C., Witwer, K.W., Aikawa, E., Alcaraz, M.J., Anderson, J.D., Andriantsitohaina, R., Antoniou, A., Arab, T., Archer, F., Atkin-Smith, G.K., et al. (2018). Minimal information for studies of extracellular vesicles 2018 (MISEV2018): a position statement of the International Society for Extracellular Vesicles and update of the MISEV2014 guidelines. *J. Extracell. Vesicles* 7, 1535750.
  36. Kowal, J., Arras, G., Colombo, M., Jouve, M., Morath, J.P., Primdal-Bengtson, B., Dingli, F., Loew, D., Tkach, M., and Théry, C. (2016). Proteomic comparison defines novel markers to characterize heterogeneous populations of extracellular vesicle subtypes. *Proc. Natl. Acad. Sci. USA* 113, E968–E977.
  37. Michalik, K.M., You, X., Manavski, Y., Doddaballapur, A., Zörnig, M., Braun, T., John, D., Ponomareva, Y., Chen, W., Uchida, S., et al. (2014). Long noncoding RNA MALAT1 regulates endothelial cell function and vessel growth. *Circ. Res.* 114, 1389–1397.
  38. Vausort, M., Wagner, D.R., and Devaux, Y. (2014). Long noncoding RNAs in patients with acute myocardial infarction. *Circ. Res.* 115, 668–677.
  39. Wang, Y.-N.-Z., Shan, K., Yao, M.-D., Yao, J., Wang, J.-J., Li, X., Liu, B., Zhang, Y.-Y., Ji, Y., Jiang, Q., and Yan, B. (2016). Long noncoding RNA-GAS5: a novel regulator of hypertension-induced vascular remodeling. *Hypertension* 68, 736–748.
  40. Yin, Q., Wu, A., and Liu, M. (2017). Plasma Long Non-Coding RNA (lncRNA) GAS5 is a New Biomarker for Coronary Artery Disease. *Med. Sci. Monit.* 23, 6042–6048.
  41. Kurian, L., Aguirre, A., Sancho-Martinez, I., Benner, C., Hishida, T., Nguyen, T.B., Reddy, P., Nivet, E., Krause, M.N., Nelles, D.A., et al. (2015). Identification of novel long noncoding RNAs underlying vertebrate cardiovascular development. *Circulation* 131, 1278–1290.
  42. Pan, J.X. (2017). LncRNA H19 promotes atherosclerosis by regulating MAPK and NF- $\kappa$ B signaling pathway. *Eur. Rev. Med. Pharmacol. Sci.* 21, 322–328.
  43. Bitarafan, S., Yari, M., Broumand, M.A., Ghaderian, S.M.H., Rahimi, M., Mirfakhraie, R., Azizi, F., and Omrani, M.D. (2019). Association of Increased Levels of lncRNA H19 in PBMCs with Risk of Coronary Artery Disease. *Cell J.* 20, 564–568.
  44. Bei, Y., Das, S., Rodosthenous, R.S., Holvoet, P., Vanhaverbeke, M., Monteiro, M.C., Monteiro, V.V.S., Radosinska, J., Bartekova, M., Jansen, F., et al. (2017). Extracellular Vesicles in Cardiovascular Theranostics. *Theranostics* 7, 4168–4182.
  45. Ge, Q., Zhou, Y., Lu, J., Bai, Y., Xie, X., and Lu, Z. (2014). miRNA in plasma exosome is stable under different storage conditions. *Molecules* 19, 1568–1575.
  46. Juni, R.P., Abreu, R.C., and da Costa Martins, P.A. (2017). Regulation of microvascularization in heart failure - an endothelial cell, non-coding RNAs and exosome liaison. *Noncoding RNA Res.* 2, 45–55.
  47. Mehta, J.L., Saldeen, T.G., and Rand, K. (1998). Interactive role of infection, inflammation and traditional risk factors in atherosclerosis and coronary artery disease. *J. Am. Coll. Cardiol.* 31, 1217–1225.
  48. Zhang, C., Xu, X., Potter, B.J., Wang, W., Kuo, L., Michael, L., Bagby, G.J., and Chilian, W.M. (2006). TNF- $\alpha$  contributes to endothelial dysfunction in ischemia/reperfusion injury. *Arterioscler. Thromb. Vasc. Biol.* 26, 475–480.
  49. Pirillo, A., Norata, G.D., and Catapano, A.L. (2013). LOX-1, OxLDL, and atherosclerosis. *Mediators Inflamm.* 2013, 152786.
  50. Li, D., and Mehta, J.L. (2005). Oxidized LDL, a critical factor in atherogenesis. *Cardiovasc. Res.* 68, 353–354.
  51. Sitia, S., Tomasoni, L., Atzeni, F., Ambrosio, G., Cordiano, C., Catapano, A., Tramontana, S., Perticone, F., Naccarato, P., Camici, P., et al. (2010). From endothelial dysfunction to atherosclerosis. *Autoimmun. Rev.* 9, 830–834.
  52. Villarroya-Beltri, C., Gutiérrez-Vázquez, C., Sánchez-Cabo, F., Pérez-Hernández, D., Vázquez, J., Martín-Cofreces, N., Martínez-Herrera, D.J., Pascual-Montano, A., Mittelbrunn, M., and Sánchez-Madrid, F. (2013). Sumoylated hnRNPA2B1 controls the sorting of miRNAs into exosomes through binding to specific motifs. *Nat. Commun.* 4, 2980.
  53. Qu, L., Ding, J., Chen, C., Wu, Z.J., Liu, B., Gao, Y., Chen, W., Liu, F., Sun, W., Li, X.F., et al. (2016). Exosome-Transmitted lncARSR Promotes Sunitinib Resistance in Renal Cancer by Acting as a Competing Endogenous RNA. *Cancer Cell* 29, 653–668.
  54. Zietzer, A., Hosen, M.R., Wang, H., Goody, P.R., Sylvester, M., Latz, E., Nickenig, G., Werner, N., and Jansen, F. (2020). The RNA-binding protein hnRNPU regulates the sorting of microRNA-30c-5p into large extracellular vesicles. *J. Extracell. Vesicles* 9, 1786967.
  55. Janas, T., Janas, M.M., Sapoń, K., and Janas, T. (2015). Mechanisms of RNA loading into exosomes. *FEBS Lett.* 589, 1391–1398.
  56. Agostini, F., Zanzoni, A., Klus, P., Marchese, D., Cirillo, D., and Tartaglia, G.G. (2013). catRAPID omics: a web server for large-scale prediction of protein-RNA interactions. *Bioinformatics* 29, 2928–2930.
  57. Lin, Y., Liu, T., Cui, T., Wang, Z., Zhang, Y., Tan, P., Huang, Y., Yu, J., and Wang, D. (2020). RNAInter in 2020: RNA interactome repository with increased coverage and annotation. *Nucleic Acids Res.* 48 (D1), D189–D197.
  58. Bateman, A., Agrawal, S., Birney, E., Bruford, E.A., Bujnicki, J.M., Cochrane, G., Cole, J.R., Dinger, M.E., Enright, A.J., Gardner, P.P., et al. (2011). RNAcentral: A vision for an international database of RNA sequences. *RNA* 17, 1941–1946.
  59. Bonnici, V., Caro, G., Constantino, G., Liuni, S., D’Elia, D., Bombieri, N., Licciulli, F., and Giugno, R. (2018). Arena-Idb: a platform to build human non-coding RNA interaction networks. *BMC Bioinformatics* 19 (Suppl 10), 350.
  60. Yang, J., Li, C., Zhang, L., and Wang, X. (2018). Extracellular Vesicles as Carriers of Non-coding RNAs in Liver Diseases. *Front. Pharmacol.* 9, 415.
  61. Hobor, F., Dallmann, A., Ball, N.J., Cicchini, C., Battistelli, C., Ogradowicz, R.W., Christodoulou, E., Martin, S.R., Castello, A., Tripodi, M., et al. (2018). A cryptic RNA-binding domain mediates SyncrIP recognition and exosomal partitioning of miRNA targets. *Nat. Commun.* 9, 831.

62. Shibuya, M. (2011). Vascular Endothelial Growth Factor (VEGF) and Its Receptor (VEGFR) Signaling in Angiogenesis: A Crucial Target for Anti- and Pro-Angiogenic Therapies. *Genes Cancer* 2, 1097–1105.
63. Xu, Y., Wu, W., Han, Q., Wang, Y., Li, C., Zhang, P., and Xu, H. (2019). Post-translational modification control of RNA-binding protein hnRNPK function. *Open Biol.* 9, 180239.
64. Wang, Z., Qiu, H., He, J., Liu, L., Xue, W., Fox, A., Tickner, J., and Xu, J. (2020). The emerging roles of hnRNPK. *J. Cell. Physiol.* 235, 1995–2008.
65. Leal, G., Comprido, D., de Luca, P., Morais, E., Rodrigues, L., Mele, M., Santos, A.R., Costa, R.O., Pinto, M.J., Patil, S., et al. (2017). The RNA-binding protein hnRNP K mediates the effect of BDNF on dendritic mRNA metabolism and regulates synaptic NMDA receptors in hippocampal neurons. *eNeuro* 4, ENEURO.0268-17.2017.
66. Yoon, Y., McKenna, M.C., Rollins, D.A., Song, M., Nuriel, T., Gross, S.S., Xu, G., and Glatt, C.E. (2013). Anxiety-associated alternative polyadenylation of the serotonin transporter mRNA confers translational regulation by hnRNPK. *Proc. Natl. Acad. Sci. USA* 110, 11624–11629.
67. Van Roosbroeck, K., Pollet, J., and Calin, G.A. (2013). miRNAs and long noncoding RNAs as biomarkers in human diseases. *Expert Rev. Mol. Diagn.* 13, 183–204.
68. Kim, K.M., Abdelmohsen, K., Mustapic, M., Kapogiannis, D., and Gorospe, M. (2017). RNA in extracellular vesicles. *Wiley Interdiscip. Rev. RNA* 8, e1413.
69. Jansen, F., Yang, X., Proebsting, S., Hoelscher, M., Przybilla, D., Baumann, K., Schmitz, T., Dolf, A., Endl, E., Franklin, B.S., et al. (2014). MicroRNA expression in circulating microvesicles predicts cardiovascular events in patients with coronary artery disease. *J. Am. Heart Assoc.* 3, e001249.
70. Fritz, J.V., Heintz-Buschart, A., Ghosal, A., Wampach, L., Etheridge, A., Galas, D., and Wilmes, P. (2016). Sources and Functions of Extracellular Small RNAs in Human Circulation. *Annu. Rev. Nutr.* 36, 301–336.
71. Mateescu, B., Kowal, E.J., van Balkom, B.W., Bartel, S., Bhattacharyya, S.N., Buzás, E.I., Buck, A.H., de Candia, P., Chow, F.W., Das, S., et al. (2017). Obstacles and opportunities in the functional analysis of extracellular vesicle RNA - an ISEV position paper. *J. Extracell. Vesicles* 6, 1286095.
72. Dong, L., Lin, W., Qi, P., Xu, M.D., Wu, X., Ni, S., Huang, D., Weng, W.W., Tan, C., Sheng, W., et al. (2016). Circulating long RNAs in serum extracellular vesicles: their characterization and potential application as biomarkers for diagnosis of colorectal cancer. *Cancer Epidemiol. Biomarkers Prev.* 25, 1158–1166.
73. Busch, A., Eken, S.M., and Maegdefessel, L. (2016). Prospective and therapeutic screening value of non-coding RNA as biomarkers in cardiovascular disease. *Ann. Transl. Med.* 4, 236.
74. Cai, Y., Yang, Y., Chen, X., Wu, G., Zhang, X., Liu, Y., Yu, J., Wang, X., Fu, J., Li, C., et al. (2016). Circulating 'lncRNA OTTHUMT00000387022' from monocytes as a novel biomarker for coronary artery disease. *Cardiovasc. Res.* 112, 714–724.
75. Yu, B., and Wang, S. (2018). Angio-LncRs: LncRNAs that regulate angiogenesis and vascular disease. *Theranostics* 8, 3654–3675.
76. Aryal, B., Rotllan, N., and Fernández-Hernando, C. (2014). Noncoding RNAs and atherosclerosis. *Curr. Atheroscler. Rep.* 16, 407.
77. Guduric-Fuchs, J., O'Connor, A., Camp, B., O'Neill, C.L., Medina, R.J., and Simpson, D.A. (2012). Selective extracellular vesicle-mediated export of an overlapping set of microRNAs from multiple cell types. *BMC Genomics* 13, 357.
78. Mathieu, M., Martin-Jaular, L., Lavieu, G., and Théry, C. (2019). Specificities of secretion and uptake of exosomes and other extracellular vesicles for cell-to-cell communication. *Nat. Cell Biol.* 21, 9–17.
79. Li, X., Liu, R., Huang, Z., Gurley, E.C., Wang, X., Wang, J., He, H., Yang, H., Lai, G., Zhang, L., et al. (2018). Cholangiocyte-derived exosomal long noncoding RNA H19 promotes cholestatic liver injury in mouse and humans. *Hepatology* 68, 599–615.
80. Kong, L., Zhang, Y., Ye, Z.Q., Liu, X.Q., Zhao, S.Q., Wei, L., and Gao, G. (2007). CPC: assess the protein-coding potential of transcripts using sequence features and support vector machine. *Nucleic Acids Res.* 35 (Suppl 2), W345–W349.
81. Jansen, F., Yang, X., Hoelscher, M., Cattelan, A., Schmitz, T., Proebsting, S., Wenzel, D., Vosen, S., Franklin, B.S., Fleischmann, B.K., et al. (2013). Endothelial microparticle-mediated transfer of MicroRNA-126 promotes vascular endothelial cell repair via SPRED1 and is abrogated in glucose-damaged endothelial microparticles. *Circulation* 128, 2026–2038.
82. Jansen, F., Zietzer, A., Stumpf, T., Flender, A., Schmitz, T., Nickenig, G., and Werner, N. (2017). Endothelial microparticle-promoted inhibition of vascular remodeling is abrogated under hyperglycaemic conditions. *J. Mol. Cell. Cardiol.* 112, 91–94.
83. Théry, C., Amigorena, S., Raposo, G., and Clayton, A. (2006). Isolation and characterization of exosomes from cell culture supernatants and biological fluids. *Curr. Protoc. Cell Biol.*, Chapter 3, Unit 3.22.
84. Tkach, M., Kowal, J., Zucchetti, A.E., Enserink, L., Jouve, M., Lankar, D., Saitakis, M., Martin-Jaular, L., and Théry, C. (2017). Qualitative differences in T-cell activation by dendritic cell-derived extracellular vesicle subtypes. *EMBO J.* 36, 3012–3028.

OMTN, Volume 25

## Supplemental information

**CAD increases the long noncoding RNA *PUNISHER*  
in small extracellular vesicles and regulates  
endothelial cell function via vesicular shuttling**

**Mohammed Rabiul Hosen, Qian Li, Yangyang Liu, Andreas Zietzer, Katharina Maus, Philip Goody, Shizuka Uchida, Eicke Latz, Nikos Werner, Georg Nickenig, and Felix Jansen**

### **Primers for Taqman RT-qPCR**

Taqman RT-qPCR primers: *MALAT1* (Hs01910177\_s1, Thermo Fisher Scientific); *GAS5* (Hs05021116\_g1, Thermo Fisher Scientific); *H19* (Hs00399294\_g1, Thermo Fisher Scientific); *PUNISHER* (Hs01096080\_s1, Thermo Fisher Scientific); *VEGFA* (Hs00900055\_m1, Thermo Fisher Scientific); *hnRNPK* (Hs03989611\_gH, Thermo Fisher Scientific), and *GAPDH* (Hs02758991\_g1, Thermo Fisher Scientific).

### **Antibodies for western blotting**

Primary antibodies used: anti-CD81 (1:1000; Santa Cruz, #sc-166029); anti-CD9 (1:1000; Cell Signaling Technology, #13403); anti-Syntenin1 (1:1000; Abcam, #ab133267); anti-albumin (1:2000; Abcam, #ab10241); anti- $\beta$ -Actin (1:2500; Sigma-Aldrich, #A1978); anti-hnRNPK (1:1000; Abcam, #ab39975); anti-VEGFA (1:1000; Novus Biologicals, #NB100-2381); anti-Histone H3 (1:1000; Abcam, #1791). Secondary antibodies used: anti-Rabbit IgG (1:1000; Sigma-Aldrich, #A9169) or anti-Mouse IgG (1:3000; Sigma-Aldrich, #A9044).

### **siRNAs for EC knockdown**

All siRNAs used in these studies were purchased from Thermo Fisher Scientific: *PUNISHER* siRNA (Assay ID: n272074, Thermo Fisher Scientific), *hnRNPK* siRNA (Assay ID: s6737, Thermo Fisher Scientific), or control siRNA (#AM4611, Thermo Fisher Scientific).

### **Proliferation assay by fluorescence microscopy**

Bromodeoxyuridine (BrdU; 10  $\mu$ M stock solution, BD Biosciences, #550891) was added to the cell medium and cultured for 6 hours. ECs were fixed and denatured, followed by the detection of BrdU incorporation using rat anti-BrdU antibody (Abcam, #ab6326) and anti-rat-Cy3 (Jackson ImmunoResearch, #712-165-150) secondary antibody. Nuclei were counterstained with DAPI

(Vector laboratories, #H-1500-10). A Zeiss Axiovert 200M microscope and ZEN 2.3 pro software were used to take images.

### **Spheroid sprouting assays**

Spheroid assays were performed as previously described<sup>1</sup>. *In vitro* angiogenesis was quantified by measuring the cumulative length of all sprouts of each spheroid or the maximal distance of the migrated cells using digital imaging analysis software (AxioVision Rel. 4.8, Carl Zeiss). 10 spheroids were analyzed for each experiment.

### **Nanoparticle tracking analysis**

Size and concentration distribution of plasma sEVs and endothelial sEVs were performed by using nanoparticle tracking analysis (NTA) with a Nanosight NS 300 (Malvern Instruments, UK). Each sample was recorded 5 times for 60 seconds at a speed level of 20. The analysis was performed by setting a detection threshold of 6. PBS was used to perform a background measurement, in order to confirm the absence of residual particles. The NTA software (version 3.1 Build 3.1.46) was used to record and analyze the samples.

### **Absolute RT-qPCR analysis of *PUNISHER* expression**

The absolute expression of *PUNISHER* was determined by using a standard-curve method with a plasmid containing the *PUNISHER* sequence, GenScript, vector name: pUC57, length: 201bp.

The plasmid sequence is shown here:

```
5'-ACGGCGGCCACAGCTGGCGGCCAGCGGCTCCTCCGAGGTGCTCAGCGGCCAG  
GAACAGTAGCTGCTCGTACTTGGCGCGAATCCACGACTCGCGCTCCTCCCTGCAAGACC  
AGGGATCAACGGAAAAGGCTCTAGGGACCCCCAGCCAGGACTTCTGCCCCTACCCACGG  
GACCGTCTCAGGTTTCGCACACCCTCAG-3'
```

### **Subcellular fractionation of RNA**

Fractionation of nuclear and cytoplasmic RNA was carried out with the cytoplasmic and nuclear RNA purification kit (Norgen Biotek, #21000), strictly following the manufacturer's protocol. RNA quality and concentration were assessed using a NanoDrop 2000 (Thermo Fisher Scientific). To isolate nuclear and cytoplasmic RNAs, ECs were washed once with 1xPBS and detached from the dish. After two washes with ice-cold PBS, pellets were resuspended in 200  $\mu$ l of Buffer A (10 mM Tris pH=8; 140 mM NaCl; 1.5 mM MgCl<sub>2</sub>; and 0.5% Nonidet P-40) and incubated on ice for 5 min, with gentle flicking of the tube every 90 sec. Following incubation, the suspension was centrifuged at 1000xg at 4°C for 3 min. The supernatant (containing the cytoplasmic fraction) was collected and loaded onto spin columns, according to manufacturer's protocol. The cell pellet was washed twice with Buffer A and resuspended in Buffer B (Buffer A + 1% Tween-40; 0.5% deoxycholate). After centrifugation at 1000xg at 4°C for 3 min, the supernatant was discarded. The pellet (containing nuclei) was resuspended in Buffer B and processed in order to obtain nuclear fractions.

### **Subcellular fractionation of protein**

Protein extraction from nucleoplasm and cytoplasm was conducted with the NE-PER Nuclear and Cytoplasmic Extraction Reagents (Thermo Fisher Scientific, #78833) by following the manufacturer's protocol. ECs were detached with a solution of trypsin-EDTA and then centrifuged at 500xg for 5 minutes. The cells were resuspended in PBS, counted, and then  $8 \times 10^6$  cells were centrifuged at 500xg for 3 minutes. The supernatant was discarded and the cell pellets were dried. The dried pellet was resuspended with 500  $\mu$ l ice-cold Cytoplasmic Extraction Reagent I (CER I), then the tube was incubated on ice for 10 minutes. Following this,

27.5 µl ice-cold Cytoplasmic Extraction Reagent II (CER II) was added and incubated on ice for 1 minute. The tube was then centrifuged at 16,000×g for 5 minutes. The supernatant (cytoplasmic extract) was transferred to a clean pre-chilled tube and stored at -80°C until it was used. Finally, the nuclear pellet was resuspended in ice-cold Nuclear Extraction Reagent (NER). The sample was vortexed for 15 seconds every 10 minutes, for a total of 40 minutes. The pellet was centrifuged at 16,000×g for 10 minutes. The supernatant (nuclear extract) was transferred to a pre-chilled tube and then stored at -80°C until it was used.

### **Immunocytochemical staining**

Immunocytochemistry of ECs (ECs) was performed by using anti-hnRNPk antibody (Abcam, #ab39975) and Phalloidin–Atto 594 (Sigma-Aldrich, #51927-10NMOL).  $3 \times 10^4$  ECs per well were grown in a 4-well chamber slide (Milipore, #PEZGS0416). Twenty-four hours after seeding, cells were rinsed with PBS and fixed with 4% paraformaldehyde in PBS for 10 min at RT. Fixed cells were washed with PBS and incubated with 0.25% Triton X-100 (Sigma-Aldrich) in PBS for 10 min at RT for permeabilization of the cell membranes. After three washing steps with PBS, cells were incubated with the blocking solution (0.25% Triton X-100; 1% bovine serum albumin (BSA) in PBS) for 1 hour at RT. Subsequently, cells were incubated with anti-hnRNPk antibody (1:500) in the blocking solution overnight at 4°C. After extensive washing with PBS, the cells were incubated with Alexa Fluor-488 conjugated secondary antibody (Thermo Fisher Scientific) and Phalloidin–Atto 594 (Sigma-Aldrich, 51927-10NMOL) for 60 min at RT. After washing with PBS, DAPI (Sigma-Aldrich) staining was applied and the chamber slide was mounted by using ProLong Gold Antifade (Invitrogen, P36941). Images were taken with a Zeiss Axio Observer inverted microscope and analyzed with the ZEN 2.3 pro software.

### **Scratch-wound assay**

A scratch wound was made in the middle of the culture dish with a sterile p10 pipette tip. Cell migration was observed by capturing bright-field images of the dish at different time points (0, 4, 8, and 12 hours). The tendency of cells to migrate towards the scratch was measured by using digital image analysis software (AxioVision Rel.4.8, Carl Zeiss). The rate of migration was calculated by quantifying the total distance covered by the cells from the edge of the scratch toward the center of the scratch.

### **Boyden chamber assay**

$1 \times 10^5$  ECs were seeded onto the upper compartment of a Boyden chamber (BD Falcon) with trans-well polycarbonate inserts (8.0  $\mu\text{m}$  pore size) and the cells were allowed to migrate for 4 hours. Following this incubation, cells on the upper side of the insert were scraped off with a cotton swab. The inserts were fixed with 4% paraformaldehyde following staining with DAPI (Vector laboratories, #H-1500-10). Cell migration was quantified by counting cells from three randomly selected fields from each well.

### **EXOCET exosome quantitation assay**

The exosome concentration was measured by using an EXOCET Exosome Quantitation Kit (System Biosciences, EXOCET96A-1), according to the manufacturer's protocol. Briefly, sEVs were first lysed with exosome lysis buffer, and then the esterase activity of cholesteryl ester transfer protein (CETP) was measured with an Infinite M200 Microplate reader (Tecan) at a wavelength of 405 nm.



**Table S1. Representative samples of RNA purity**

Sample	Concentration (ng/ $\mu$ l)	260/280	260/230
Plasma-sEV-1	38.3	1.86	1.18
Plasma-sEV-2	19.5	1.95	1.93
Plasma-sEV-3	19.3	1.92	1.18
Plasma-sEV-4	15.4	1.93	1.33
Plasma-sEV-5	24.3	1.99	1.66
HCAEC-1	203.8	1.86	1.45
HCAEC-2	208.1	1.85	1.13
HCAEC-3	214.7	1.84	1.58
HCAEC-4	199.4	1.86	1.31
HCAEC-5	165.8	1.86	1.25
HCAEC-sEV-1	67.9	1.91	0.97
HCAEC-sEV-2	46.5	1.88	0.99
HCAEC-sEV-3	67.9	1.91	0.85
HCAEC-sEV-4	60.7	1.91	0.97
HCAEC-sEV-5	50	1.87	0.93

260/280. ratio of absorption at 260 nm to 280 nm; 260/230. ratio of absorption at 260 nm to 230 nm; HCAEC. human coronary artery endothelial cell; sEV. small extracellular vesicles.

**Table S2. Function and clinical relevance of selected lncRNAs in atherosclerosis**

lncRNAs	Function in Atherosclerosis	Clinical relevance	Reference
MALAT1	Promotes angiogenesis, regulates EC function	MI (peripheral blood)	42-43
GAS5	EC activation, EC proliferation, SMC phenotypic changes	CAD, Biomarker of CAD (plasma)	44-45
AGAP2-AS1 (PUNISHER)	Promotes angiogenesis, regulates EC function	Unknown	46
H19	Promotes angiogenesis, regulates EC function	CHD (serum and whole blood)	47-48

MALAT1. metastasis-associated lung adenocarcinoma transcript1; GAS5. growth arrest-specific transcript 5; PUNISHER. AGAP2 antisense RNA 1; H19. imprinted maternally expressed transcript; CAD. coronary artery disease; CHD. coronary heart disease; MI. myocardial infarction; EC. endothelial cell; SMC. smooth muscle cell.

**Table S3. Association of the level of PUNISHER with baseline characteristics**

	<b>Exp(B) (95% CI)</b>	<b>P value</b>
Age	1.071 (0.979 to 1.171)	0.068
Male sex	0.340 (0.340 to 3.446)	0.361
Arterial hypertension	0.929 (0.140 to 6.166)	0.940
Hyperlipoproteinemia	0.979 (0.181 to 5.296)	0.980
HDL	0.953 (0.881 to 1.031)	0.234
Type I diabetes	1.746 (0.106 to 28.975)	0.697
Type II diabetes	10.954 (0.386 to 311.071)	0.161
Family history	1.417 (0.190 to 10.574)	0.734
Smoking	0.435 (0.067 to 2.806)	0.381
Angiotensin Converting Enzyme inhibitors (ACEI)	0.061 (0.002 to 2.381)	0.135
Angiotensin receptor blockers (ARB)	0.035 (0.001 to 1692)	0.090
Beta blockers	4.373 (0.322 to 59.398)	0.268
Calcium channel blockers (CCB)	2.144 (0.238 to 19.330)	0.497
Diuretics	0.780 (0.127 to 4.793)	0.789
Statins	1.457 (0.078 to 27.284)	0.801
Nitrates	9.259 (0.309 to 277.466)	0.200
Clopidogrel	0.550 (0.087 to 3.485)	0.525
Aspirin	0.371 (0.021 to 6.630)	0.501

The coefficient of the continuous variables was relative to 1-U differences. Binary logistic regression according to the median of PUNISHER level; CAD. coronary artery disease; Exp(B). exponentiation of the B coefficient; HDL. high-density lipoprotein.

**Table S4. The prediction of PUNISHER–protein interaction partners**

#	Protein ID	RNA ID	Z-score	Discriminative Power (%)	Interaction Strength (%)	Domain	Motif
1	LN28B_HUMAN	NR_027032.1.HOM_1_1428-1533	-0.29	35	98	yes	yes
2	LN28B_HUMAN	NR_027032.1.HOM_1_1422-1533	-0.13	50	100	yes	yes
3	LN28B_HUMAN	NR_027032.1.HOM_1_1420-1533	-0.23	40	99	yes	yes
4	LN28B_HUMAN	NR_027032.1.HOM_1_1404-1533	-0.34	32	97	yes	yes
5	LN28B_HUMAN	NR_027032.1.HOM_1_1411-1533	-0.37	28	96	yes	yes
6	HNRNPK_HUMAN	NR_027032.1.HOM_1_1404-1533	-0.44	22	94	yes	yes
7	HNRNPK_HUMAN	NR_027032.1.HOM_1_1428-1533	-0.62	17	43	yes	yes
8	HNRNPK_HUMAN	NR_027032.1.HOM_1_1422-1533	-0.58	17	65	yes	yes
9	HNRNPK_HUMAN	NR_027032.1.HOM_1_1411-1533	-0.48	22	90	yes	yes
10	HNRNPK_HUMAN	NR_027032.1.HOM_1_1399-1533	-0.42	24	95	yes	yes
11	SRSF2_HUMAN	NR_027032.1.HOM_1_1428-1533	-0.68	14	21	yes	yes
12	HNRNPK_HUMAN	NR_027032.1.HOM_1_1420-1533	-0.59	17	60	yes	yes
13	PCBP2_HUMAN	NR_027032.1.HOM_1_1404-1533	-0.64	17	32	yes	yes
14	PCBP2_HUMAN	NR_027032.1.HOM_1_1399-1533	-0.48	22	69	yes	yes
15	SRSF2_HUMAN	NR_027032.1.HOM_1_1422-1533	-0.67	14	22	yes	yes
16	SRSF2_HUMAN	NR_027032.1.HOM_1_1420-1533	-0.64	14	31	yes	yes
17	PCBP2_HUMAN	NR_027032.1.HOM_1_1411-1533	-0.57	17	52	yes	yes
18	SRSF2_HUMAN	NR_027032.1.HOM_1_1404-1533	-0.68	14	19	yes	yes
19	PCBP2_HUMAN	NR_027032.1.HOM_1_1388-1533	-0.48	22	66	yes	yes
20	PCBP2_HUMAN	NR_027032.1.HOM_1_1420-1533	-0.71	14	24	yes	yes
21	PCBP2_HUMAN	NR_027032.1.HOM_1_1411-1533	-0.62	17	39	yes	yes
22	PCBP2_HUMAN	NR_027032.1.HOM_1_1404-1533	-0.74	14	15	yes	yes
23	SRSF2_HUMAN	NR_027032.1.HOM_1_1411-1533	-0.62	17	37	yes	yes
24	LN28B_HUMAN	NR_027032.1.HOM_1_1399-1533	-0.56	17	57	yes	yes
25	PCBP2_HUMAN	NR_027032.1.HOM_1_1420-1533	-0.74	14	15	yes	yes
26	PCBP2_HUMAN	NR_027032.1.HOM_1_1422-1533	-0.84	14	7	yes	yes
27	PCBP2_HUMAN	NR_027032.1.HOM_1_1388-1533	-0.53	20	49	yes	yes
28	PCBP2_HUMAN	NR_027032.1.HOM_1_1339-1533	-0.01	59	92	yes	yes
29	PCBP2_HUMAN	NR_027032.1.HOM_1_1335-1533	-0.06	56	85	yes	yes
30	HNRNPK_HUMAN	NR_027032.1.HOM_1_1388-1533	-0.5	20	83	yes	yes

31	PCBP2_HUMAN	NR_027032.1.HO M I 1428-1533	- 0.84	14	6	yes	yes
32	PCBP2_HUMAN	NR_027032.1.HO M I 1422-1533	- 0.86	10	4	yes	yes
33	PCBP2_HUMAN	NR_027032.1.HO M I 1380-1533	- 0.48	22	67	yes	yes
34	PCBP2_HUMAN	NR_027032.1.HO M I 1428-1533	- 0.83	14	9	yes	yes
35	PCBP2_HUMAN	NR_027032.1.HO M I 1399-1533	- 0.59	17	38	yes	yes
36	PCBP2_HUMAN	NR_027032.1.HO M I 1374-1533	- 0.36	28	77	yes	yes
37	PCBP2_HUMAN	NR_027032.1.HO M I 1365-1533	- 0.3	33	82	yes	yes
38	PCBP2_HUMAN	NR_027032.1.HO M I 1345-1533	- 0.09	54	89	yes	yes
39	HNRNPK_HUMAN	NR_027032.1.HO M I 1380-1533	- 0.48	20	86	yes	yes
40	PCBP2_HUMAN	NR_027032.1.HO M I 1374-1533	- 0.4	26	81	yes	yes
41	LN28B_HUMAN	NR_027032.1.HO M I 1388-1533	- 0.63	17	42	yes	yes
42	PCBP2_HUMAN	NR_027032.1.HO M I 1380-1533	- 0.57	17	40	yes	yes
43	PCBP2_HUMAN	NR_027032.1.HO M I 1363-1533	- 0.36	28	66	yes	yes
44	PCBP2_HUMAN	NR_027032.1.HO M I 1357-1533	- 0.44	22	51	yes	yes
45	PCBP2_HUMAN	NR_027032.1.HO M I 1348-1533	- 0.27	35	68	yes	yes
46	PCBP2_HUMAN	NR_027032.1.HO M I 1399-1533	- 0.64	14	22	yes	yes
47	PCBP2_HUMAN	NR_027032.1.HO M I 1388-1533	- 0.64	14	25	yes	yes
48	PCBP2_HUMAN	NR_027032.1.HO M I 14365-1533	- 0.45	22	68	yes	yes
49	PCBP2_HUMAN	NR_027032.1.HO M I 1380-1533	- 0.69	14	16	yes	yes
50	PCBP2_HUMAN	NR_027032.1.HO M I 1363-1533	- 0.58	17	36	yes	yes
51	PCBP2_HUMAN	NR_027032.1.HO M I 1357-1533	- 0.68	14	20	yes	yes
52	SRSF2_HUMAN	NR_027032.1.HO M I 1374-1533	- 0.6	17	45	yes	yes
53	SRSF2_HUMAN	NR_027032.1.HO M I 1357-1533	- 0.67	14	18	yes	yes
54	HNRNPK_HUMAN	NR_027032.1.HO M I 1374-1533	- 0.57	17	62	yes	yes
55	SRSF2_HUMAN	NR_027032.1.HO M I 1365-1533	- 0.58	17	42	yes	yes
56	SRSF2_HUMAN	NR_027032.1.HO M I 1363-1533	- 0.62	17	30	yes	yes
57	PCBP2_HUMAN	NR_027032.1.HO M I 1345-1533	- 0.43	24	60	yes	yes

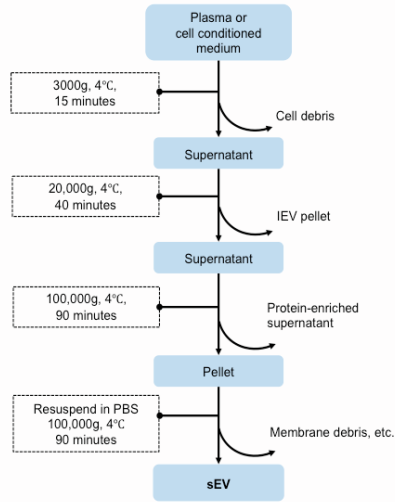
The ranking (#) of PUNISHER interaction proteins (predicted by catRAPID omics algorithm)

**Table S5. Expression of human functional long noncoding RNAs**

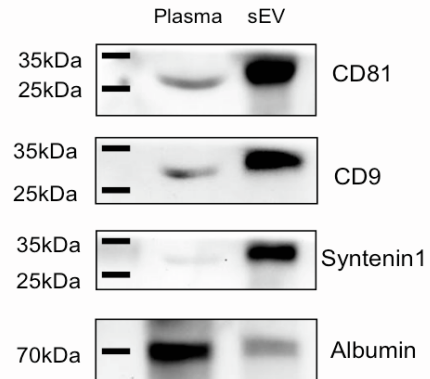
**Table S6. The prediction of RNA–protein interaction based on interaction score by RNAInter database**

## Figure S1

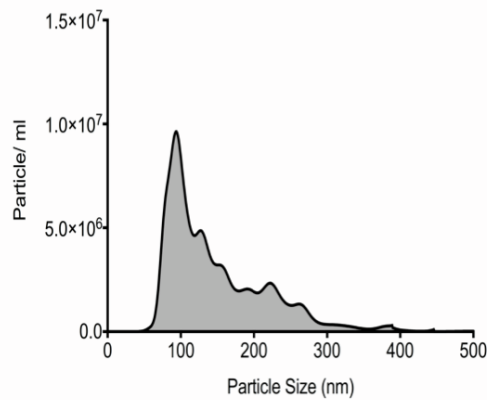
### A sEV isolation workflow



### B Immunoblotting



### C Nanoparticle Tracking Analysis (Plasma sEV)



### D Transmission Electron Microscopy (Plasma sEV)

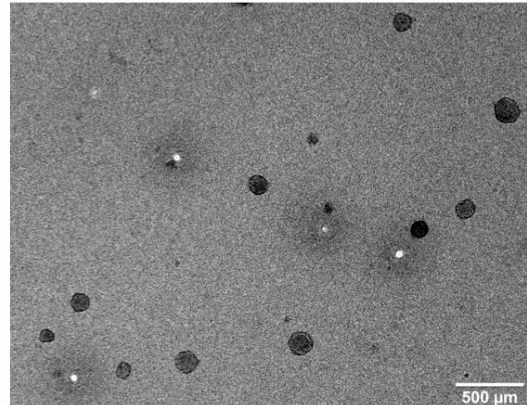


## Figure S1. Plasma sEV identification

(A) Workflow for the isolation of sEV from plasma. (B) Western-blot analysis of the expression of the sEV markers, CD81, CD9, and Syntenin1 in plasma as well as in sEV. Albumin is used as a control protein. (C) Nanoparticle tracking analysis (NTA) was used to determine the size and concentration of sEV in the plasma of patients. (D) Transmission electron microscopic (TEM) image of pelleted sEV (diameter ~30–150 nm) derived from the plasma of patients. sEV, small extracellular vesicles.

**Figure S2**

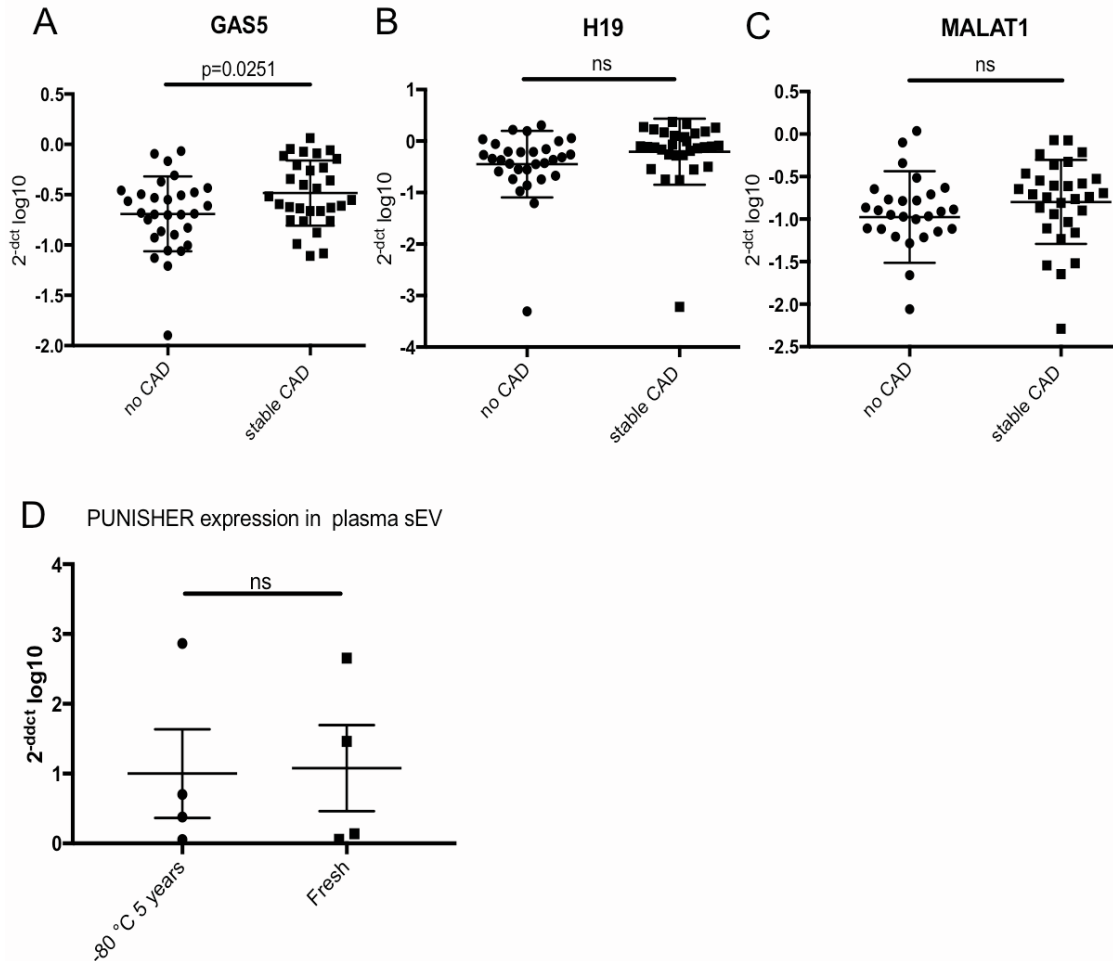


**Figure S2. Analysis of lncRNA expression in circulating sEV from patients with or without CAD**

(A-C) In the validation phase, *GAS5*, *H19*, and *MALAT1* were quantified in isolated circulating sEV from non-CAD and stable CAD patients by RT-qPCR. Values were normalized to *GAPDH* (n=30, Student t-test). (D) *PUNISHER* expression was quantified in sEV under different plasma storage conditions (ns: not significant, n=4, by Student t-test). *MALAT1*, metastasis associated lung adenocarcinoma transcript 1; CAD, coronary artery disease; sEV, small extracellular vesicles.

**Figure S3**

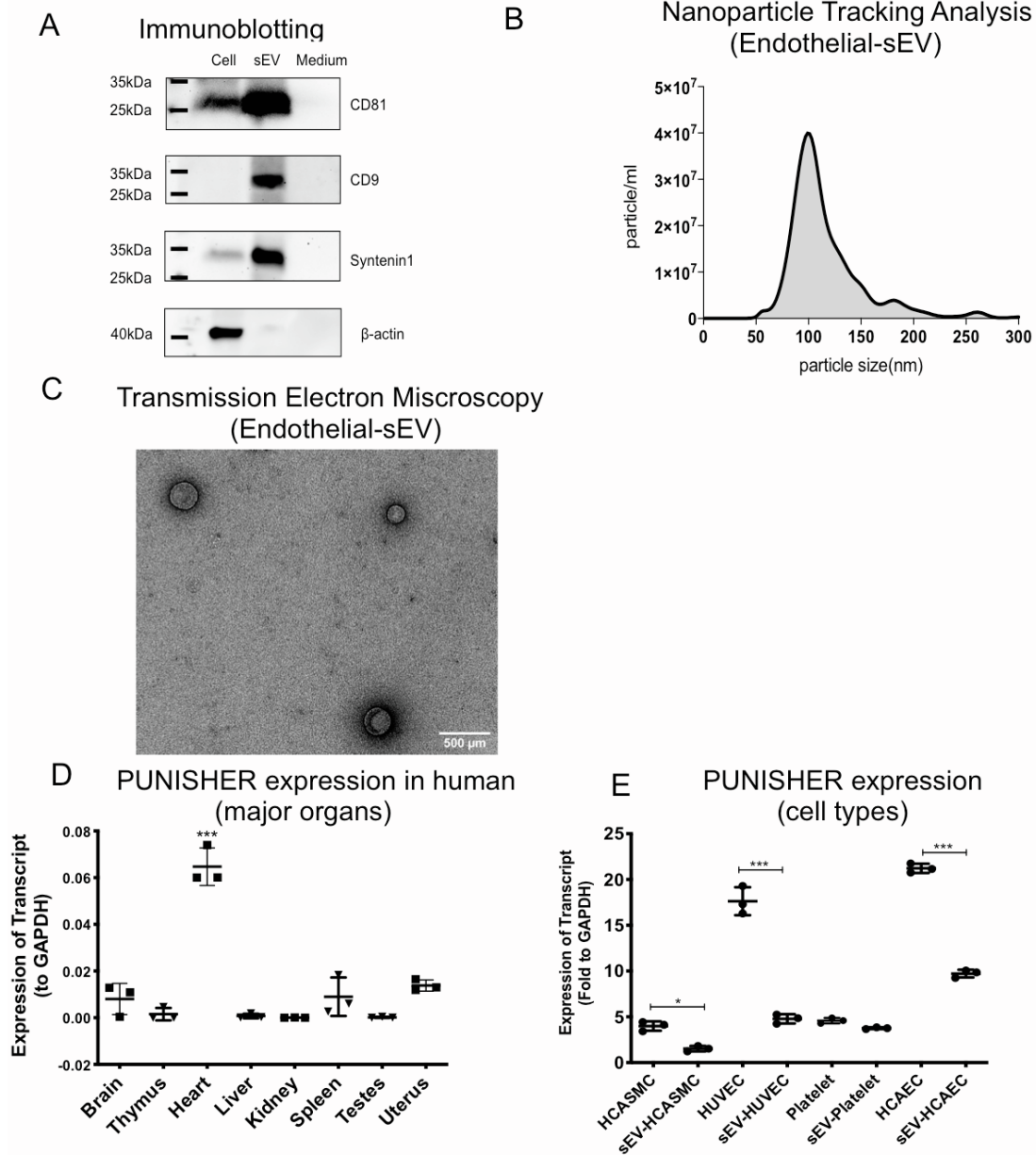


**Figure S3. Endothelial-sEV identification**

(A) Western blotting of the expression of the sEV markers (CD81, CD9, and Syntenin1) from lysed ECs, sEV, and conditioned-cell medium.  $\beta$ -Actin acts as a marker for the cell lysate. (B) Nanoparticle tracking analysis (NTA) was used to examine the size and concentration of sEV *in vitro*. (C) Transmission electron microscopic (TEM) image of pelleted sEVs (diameter ~30–150 nm) derived from ECs. (D) Expression profiling of *PUNISHER* RNA in 10 major human tissues. Results from RT-PCR by using cDNA of 10 different commercially available tissues (major organs) from humans. Purified RNA was purchased from commercial vendors as follows: Human Total RNA Master Panel II



(Clontech, #636643) (LOT NUMBER 1202050A); human heart (Amsbio, #R1234122-50, Lot No. A804058). *GAPDH* (glyceraldehyde 3-phosphate dehydrogenase) was used to normalize the data. (E) Expression of *PUNISHER* in different cell types and their corresponding sEV. (\* $p < 0.05$ , \*\*\* $p < 0.001$ ,  $n = 3$ , by Student t-test). sEV, small extracellular vesicles; EC, endothelial cells; HCASMC, human coronary artery smooth muscle cells; HUVEC, human umbilical cord endothelial cells; HCAEC, human coronary artery endothelial cells.

## Figure S4

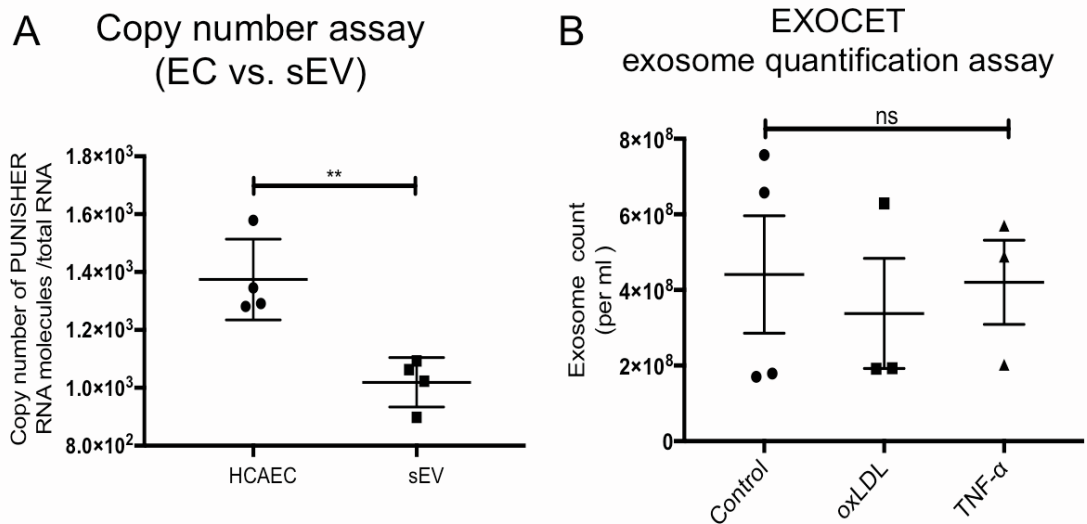


### Figure S4. Exosome quantitation assay

(A) Absolute PCR analysis (copy number assay) of *PUNISHER* in HCAECs and the corresponding sEV. ( $n = 4$ , by Student t-test). (B) EXOCET exosome quantitation assay was used to determine the exosome concentration. Parent ECs were stimulated with oxLDL, TNF- $\alpha$ , or vehicle, then sEV were isolated from the parent cells and quantified ( $n = 3$ , by 1-way ANOVA with Bonferroni's multiple comparisons test). sEV, small extracellular vesicles; ECs, endothelial cells; oxLDL, oxidized low-density lipoprotein; TNF- $\alpha$ , tumor necrosis factor alpha.

## Figure S5

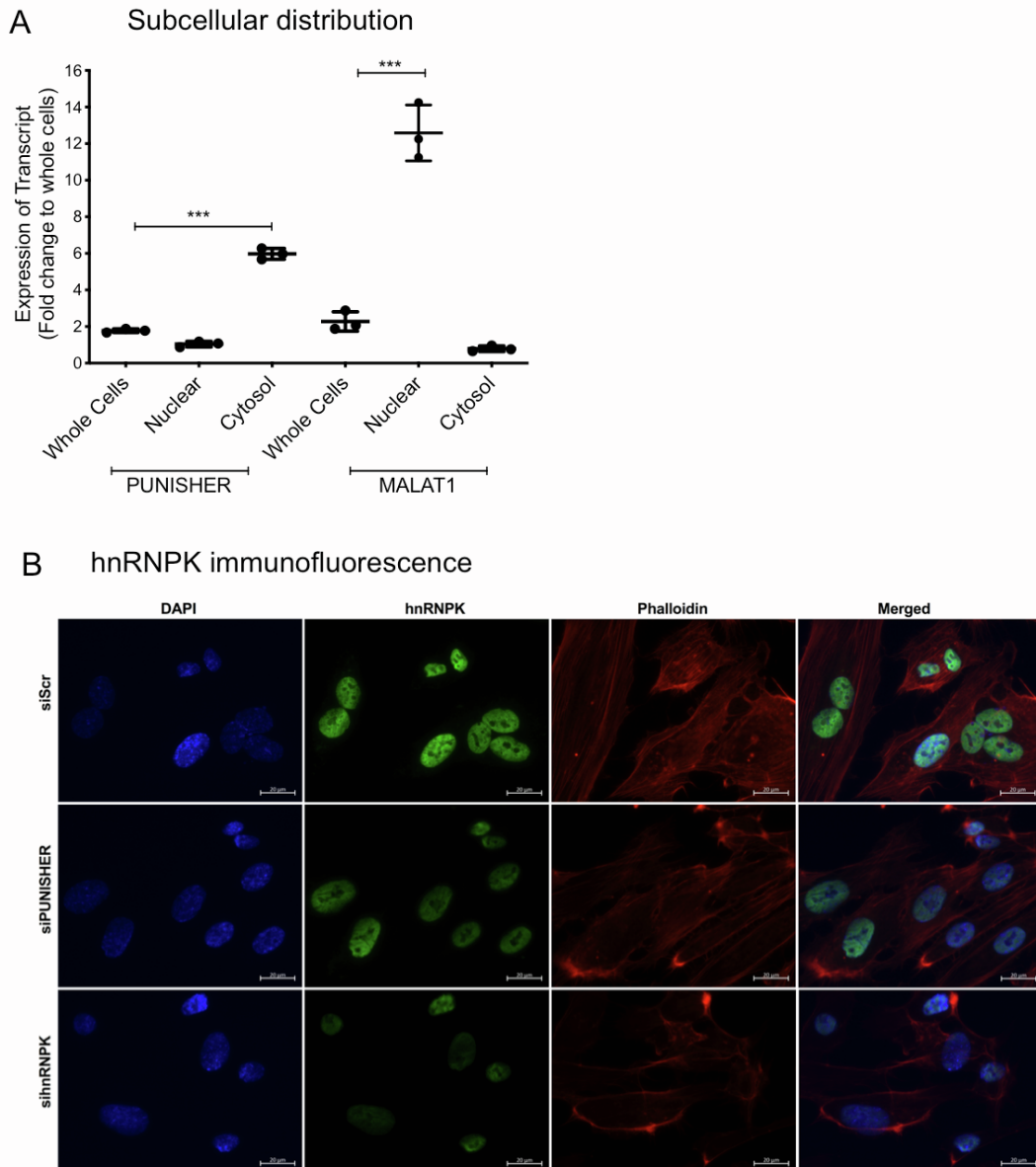


**Figure S5. Subcellular localization of PUNISHER and hnRNPk protein knockdown**  
(A) Shown is the subcellular localization of *PUNISHER* to the cytosol and nucleus, which was quantified using RT-qPCR via RNA fractionation. Interestingly, *PUNISHER* is highly enriched in the cytosol compared to the nuclear fraction of endothelial cells (HUVECs). One of the most-studied lncRNAs *MALAT1* demonstrates a predominantly nuclear localization, which was used here as a control ( $***p < 0.001$ ,  $n = 4$ , by Student t-test). lncRNA, long noncoding RNA. (B) Immunocytochemistry of hnRNPk (green), nuclear counterstaining with DAPI (blue), and F-actin staining with Phalloidin (red) in ECs confirmed the reduced expression of hnRNPk (63 $\times$ ). Upper left panel DAPI mono

staining, middle (left) Phalloidin mono staining, middle (right) hnRNPk mono staining, right panel overlay. Scale bar = 10  $\mu$ m.

**Figure S6**

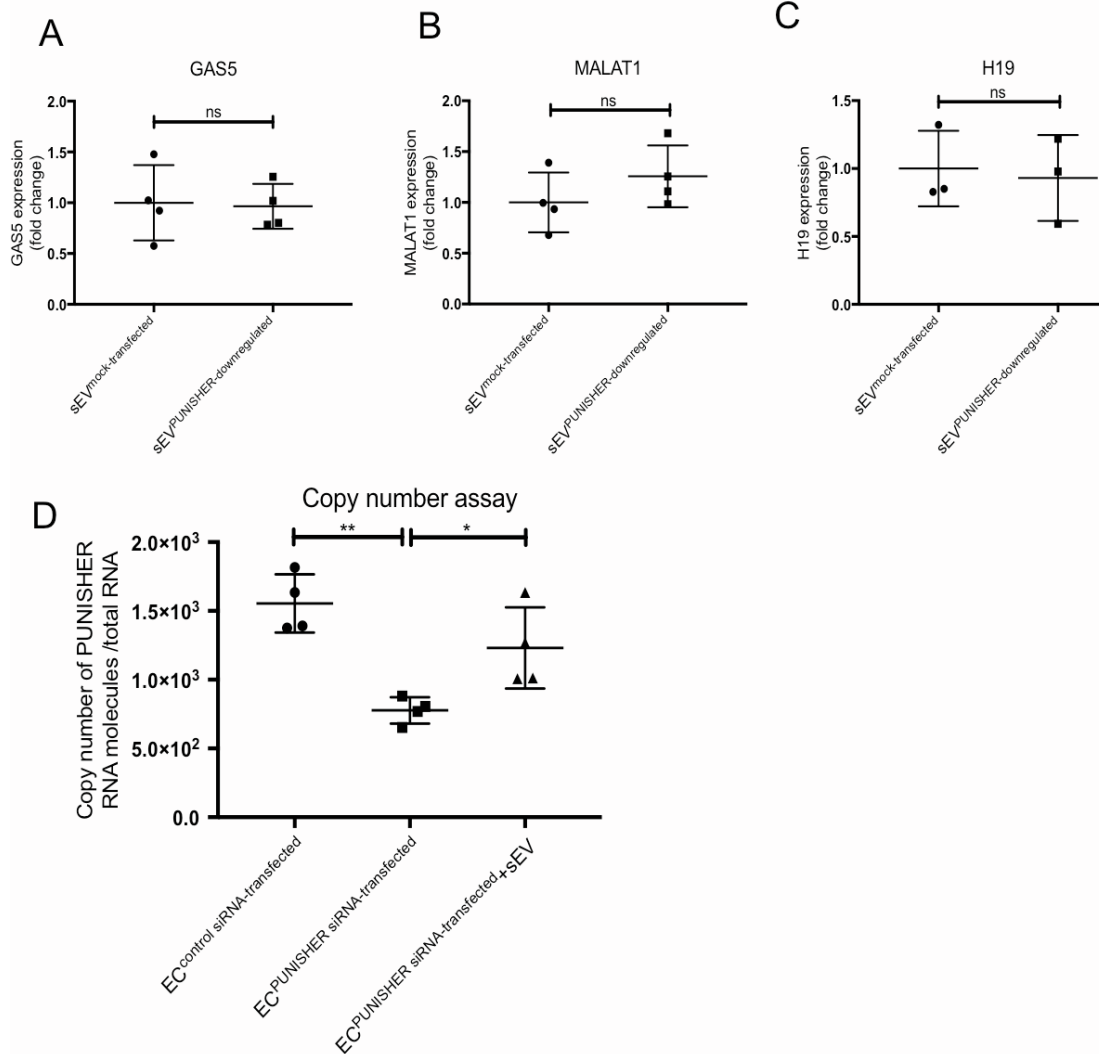


**Figure S6. lncRNA expression in sEVs**

(A-C) sEV<sup>PUNISHER-downregulated</sup> and sEV<sup>mock-transfected</sup> were separately derived from the corresponding parent ECs. *GAS5*, *MALAT1*, and *H19* were analyzed in sEV<sup>PUNISHER-downregulated</sup> and sEV<sup>mock-transfected</sup> by RT-qPCR, *GAPDH* was used as an endogenous control (n=4, by Student t-test). (D) Copy number analysis of *PUNISHER* transcripts in *PUNISHER*-downregulated recipient ECs by RT-qPCR (n=4, by Student t-test). sEV, small extracellular vesicles.

**Figure S7**

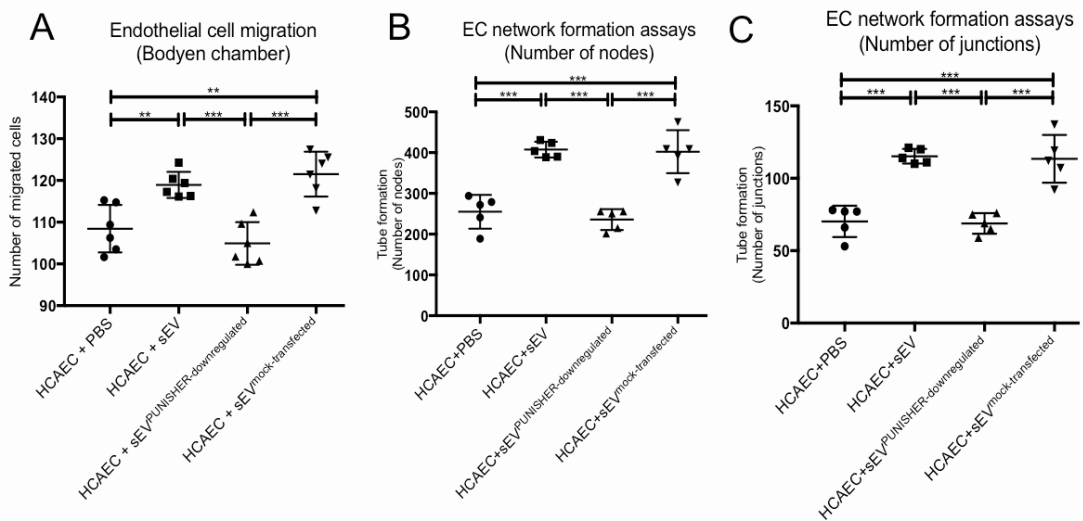


**Figure S7. Endothelial sEV-incorporated *PUNISHER* regulates the angiogenic function of target ECs**

sEV<sup>PUNISHER-downregulated</sup> and sEV<sup>mock-transfected</sup> were separately derived from parent EC. ECs in basal media were co-incubated with sEV, sEV<sup>PUNISHER-downregulated</sup>, sEV<sup>mock-transfected</sup>, or vehicle. (A) A Boyden chamber migration assay was performed on target ECs. Data are presented as the number of migrated cells (\*\* $p < 0.01$ , \*\*\* $p < 0.001$ ,  $n = 6$ , by 1-way ANOVA with Bonferroni multiple comparisons test). (B-C) ECs in basal media were co-incubated with sEV, sEV<sup>PUNISHER-downregulated</sup>, sEV<sup>mock-transfected</sup>, or vehicle. Network formation assays were performed with ECs. Capillary tubes were imaged with an immunofluorescence microscope. The number of nodes and junctions were measured and quantitated by using ImageJ image-analysis software ((B) \*\*\* $p < 0.001$ ,  $n = 5$ , by 1-way ANOVA with Bonferroni multiple comparisons test). ((C) \*\*\* $p < 0.001$ ,  $n = 6$ , by 1-way ANOVA with Bonferroni multiple comparisons test). sEV, small extracellular vesicles; ECs, endothelial cells.

**Figure S8**

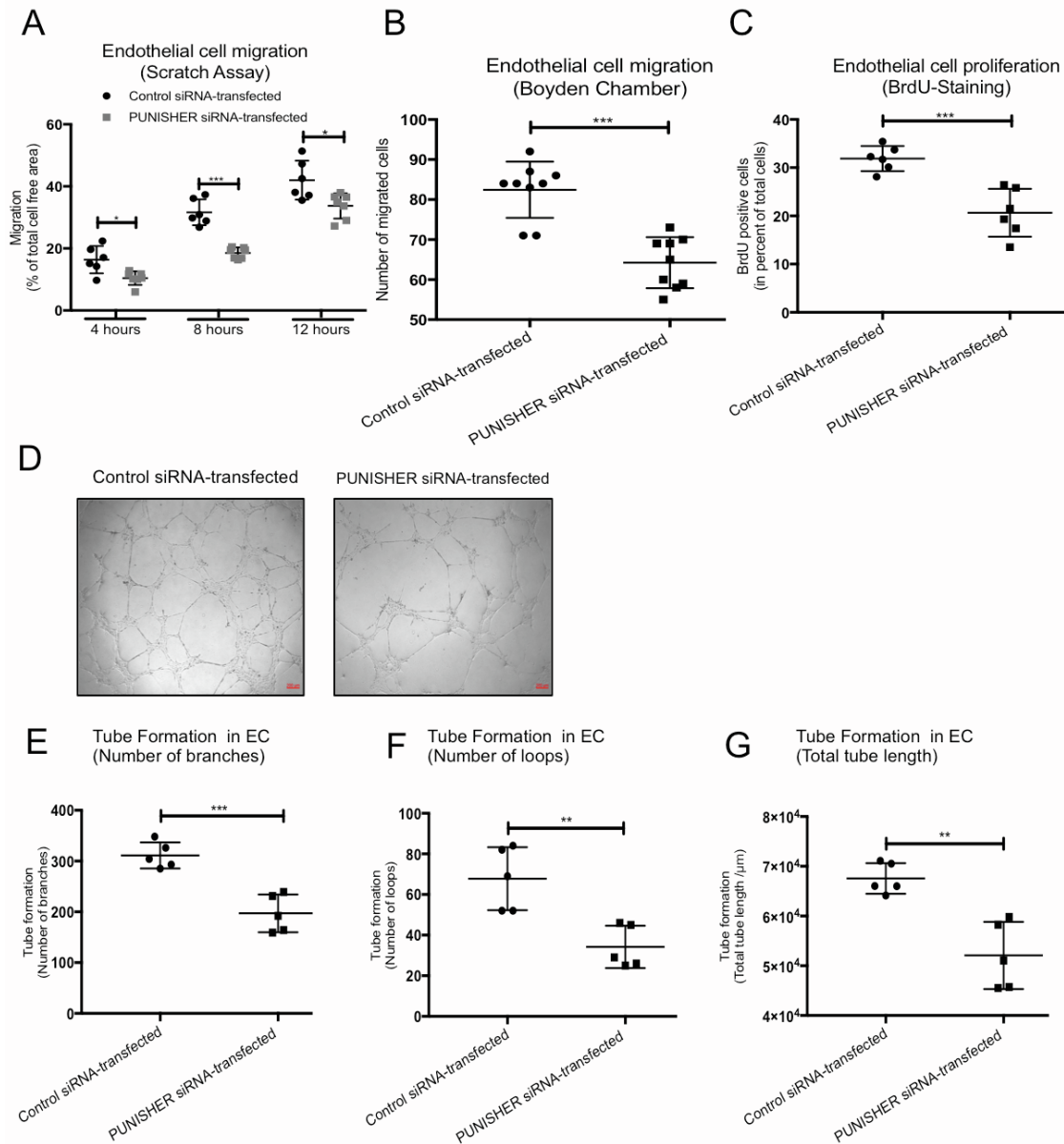


**Figure S8. *PUNISHER* promotes angiogenesis in ECs**

ECs were transfected with *PUNISHER* siRNA or control siRNA. (A) A scratch-wound assay was performed on donor ECs. Quantitative analysis of the migration of the cells was measured as a percentage of the total cell-free area ( $*p < 0.05$ ,  $***p < 0.001$ ,  $n = 6-7$ , by Student t-test). (B) A Boyden chamber assay was performed on ECs. Data are presented as the numbers of migrated cells ( $***p < 0.001$ ,  $n = 9$ , by Student t-test). (C) BrdU incorporation was determined by immunofluorescence. The percentage of BrdU-positive cells was compared with the total number of cells ( $***p < 0.001$ ,  $n = 6$ , by Student t-test). (D-G) Network formation assays in ECs. Capillary tubes were imaged with an

immunofluorescence microscope. The number of nodes, number of junctions, and total tube length were measured and quantitated by using ImageJ image-analysis software (\*\* $p < 0.01$ , \*\*\* $p < 0.001$ ,  $n = 5$ , by Student t-test). Scale bar = 200  $\mu\text{m}$ . ECs, endothelial cells.

## Figure S9

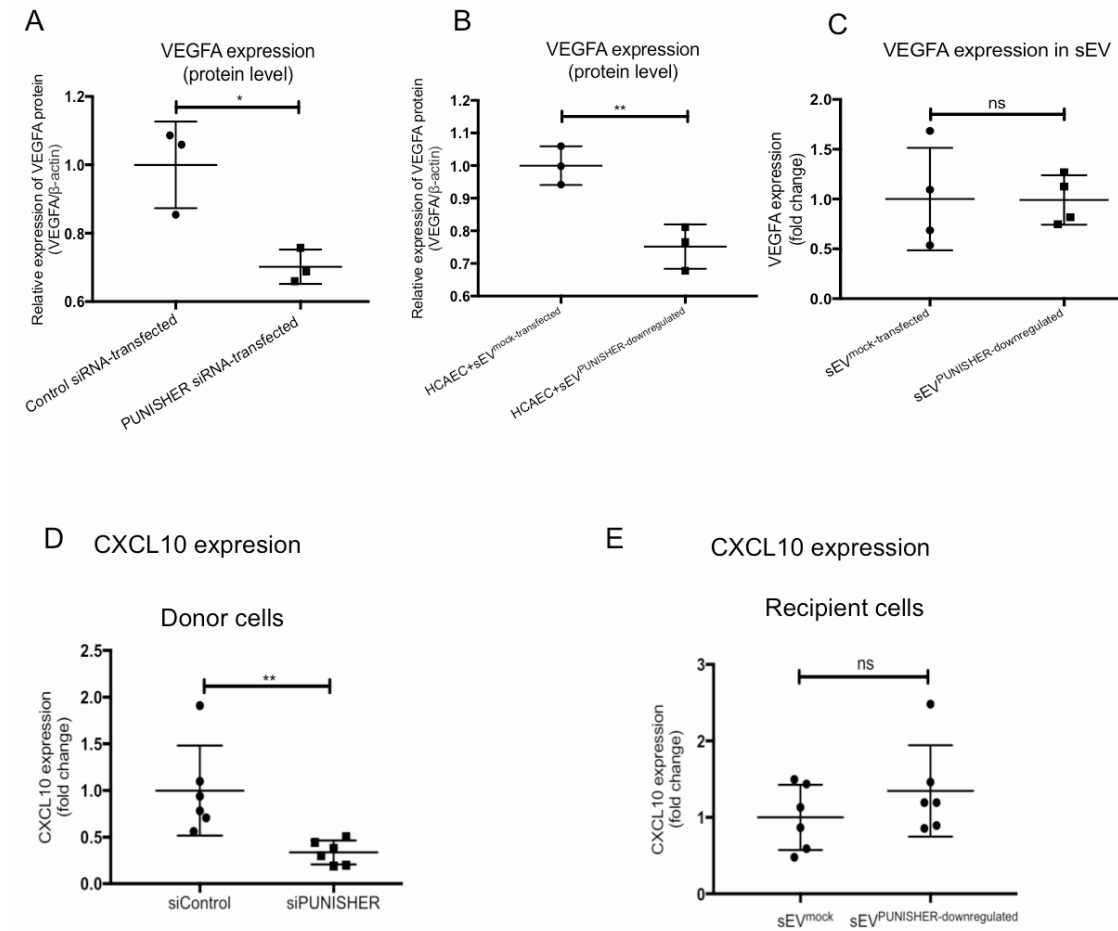
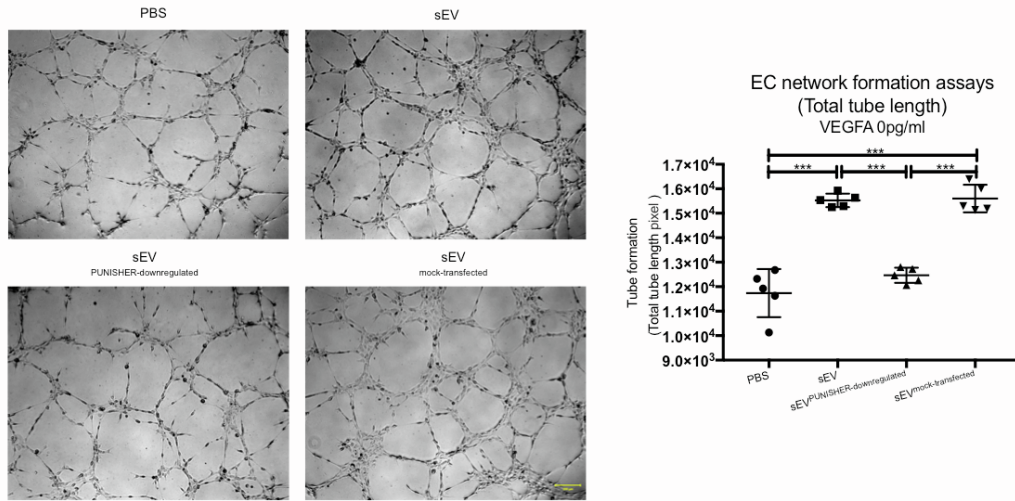


### Figure S9. *PUNISHER* controls VEGFA mRNA and protein synthesis

(A-C) VEGFA protein levels in donor or recipient ECs were quantified from western blots. (\* $p < 0.05$ , \*\* $p < 0.01$ ,  $n = 3$ , by Student t-test). (D-E) *CXCL10* expression was analyzed in donor cells after siScr and siPUNISHER treatment and in recipient cells after sEV<sup>PUNISHER-downregulated</sup> and sEV<sup>mock-transfected</sup> by RT-qPCR. *GAPDH* was used as an endogenous control (\*\* $p < 0.01$ ,  $n = 6$ , by Student t-test). sEV, small extracellular vesicles; ECs, endothelial cells; VEGFA, vascular endothelial growth factor A; CXCL10, C-X-C motif chemokine ligand 10.

**Figure S10**

**A**



**B**

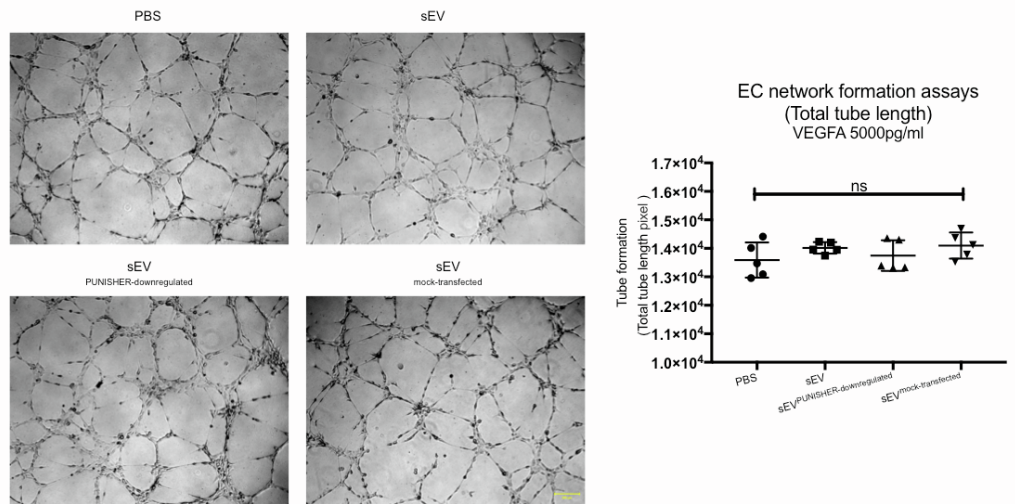


**Figure S10. Effects of *PUNISHER* can be rescued by exogenous VEGFA addition**  
ECs were transfected with *PUNISHER* siRNA or control siRNA, and the corresponding sEV were used to treat the recipient cells. (A-B) Network formation assays in ECs. Capillary tubes were imaged with an immunofluorescence microscope. Different concentrations of exogenous supplementation of VEGFA (0 pg/ml (A) or 5000 pg/ml (B)) were used. The number of nodes, number of junctions, and total tube length were measured and quantitated by using ImageJ image-analysis software (\*\*\*)  $p < 0.001$ ,  $n = 5$ , by Student t-test). Scale bar = 200  $\mu\text{m}$ . ECs, endothelial cells; VEGFA, vascular endothelial growth factor A.